Dr. rer. nat. habil. Norbert Schwarzer
Saxonian Institute of Surface Mechanics SIO
Am Lauchberg 2
04838 Eilenburg
Tel. ++49(0)3423 656639
Fax. ++49(0)3423 656666
E-Mail: n.schwarzer@siomec.de
Internet: www.siomec.de

Intrinsic stresses – Their influence on the yield strength and their measurement via nanoindentation

Abstract

It is well known that intrinsic stresses can dramatically affect the mechanical wear resistance of materials. Thus, within this work completely analytical extended Hertzian contact models for normal, tilted, sliding and rotating indenter loads will be combined with a great variety of intrinsic stress distributions in order to illustrate this effect. It will be shown that in dependence on the character and sign of the internal loads (intrinsic stresses) the load carrying capacity for distinct external contact load distributions can vary significantly. Combined with a completely analytical defect model it can be shown that this influence is even bigger in the case of repeated loading. According to the analytical model we find that, under a distinct external mechanical loading wear can be diminished or expedited in dependence on the intrinsic stress distributions.

In addition it will be shown theoretically and experimentally that measurement of intrinsic stresses should be possible via mixed load indentation experiments.

1. Introduction

Newly developed and highly sophisticated nanoindenters of "the next generation" (e.g. [1, 2] and on the more atomic scale the devices from Hysitron, ANFATEC and Asylum Research) appear to open up a wide range of combinations of the rather classical wear tests like for example scratch based test methods (pin on disc, lateral scratch etc.) with the more physical character of nanoindention experiments. The key development for closing the gap between wear tests and so called depth sensing indentation methods is the introduction of additional lateral degrees of freedom for the movement and measurement procedure of the indenter device. This leads us to depth, lateral displacement, tilting moment or even rotation angle sensing indentation methods. So, combined with classical wear test procedures one might even go so far to call this the missing experimental link for a better physical understanding of some mechanically driven wear mechanisms. However, as it is well known and will also be shown within this paper, a lot of material failure mechanisms cannot be separated from the intrinsic stresses residing in the material. Thus, the combination of intrinsic stresses and those stress fields caused by certain external loads will be the main topic of this paper.

Any kind of surface treatment, be it of chemical, mechanical or thermal kind, can cause material displacements and subsequently stresses. Also external loadings of bigger scales like for example caused by bending loads within only edge supported bars cause stresses which, with respect to additional mechanical loads of smaller scales like for example surface contacts, could be considered as "intrinsic" from the smaller scale point of view. In some cases only the inhomogeneous material structure is responsible for the occurrence of such stresses. So, e.g. intrinsic stresses within thin film-substrate compounds are mainly caused by

atomic mismatch at the interface between substrate and coating, thermal stresses resulting from the difference between deposition and room or service temperature and other effects like for example ion bombardment coming from the deposition process itself. Apart from finite element calculations dealing with the problem of intrinsic stresses (see e.g. Spaeth et al [3]) and very few somewhat more general approaches (e.g. from Finnie et al [4], Hoger [5] and Suhir [6]), the problem of intrinsic stresses has mostly been considered by using the so called "thin plate simplification", which neglects all stress components pointing in the direction of the plate normal axis. A plate-like form of the film-substrate-compound means that the total thickness, h_{tot}, is constant and small in comparison to its lateral dimensions. So, if one takes for example the z-axis as the normal axis of the coating-substrate-system one has to set:

$$\sigma_{xz} = \sigma_{yz} = \sigma_{zz} = 0. \tag{1}$$

A first consideration of the effect of intrinsic stresses came from STONEY [7] who has published a simple formula describing the bending of a coated bar in dependence on the intrinsic stress within the film. This internal stress in the film on a bar or also on a plate-like substrate causes the film-substrate compound to warp until mechanical equilibrium is reached, i.e. until both net force and bending moment are zero. From the curvature of the elastically deformed coated substrate the average film stress, σ^f, can be calculated. When the thickness of the film, h_f, is small compared to that of the substrate, the above mentioned simple formula of STONEY [7] holds. It can be given as follows:

$$\sigma_{zz}^f \approx -E_s \frac{h_s^2}{6h_f} \frac{1}{R}, \tag{2}$$

with R - radius of curvature and E_s - YOUNG´s modulus of the substrate. In those cases, where the film is not thin compared to the substrate, this formula has to be modified (e.g. [8, 9]). In its original form the STONEY formula is valid only for a narrow coated beam. The index "zz" denotes the stress component in direction of the length side of the beam which we chose to be along the z-axis. When measuring thin films deposited on plate-like substrates, the corresponding biaxial deformation has to be taken into account (see for instance [8]) by using the biaxial modulus, $E_{b,s}$, of the substrate rather than the YOUNG´s modulus alone:

$$E_s \rightarrow E_{b,s} = E_s / (1 - \nu_s) \tag{3}$$

with ν_s - POISSON´s ratio of the substrate. A very detailed discussion of these formulae and their limits is given in [9].

The knowledge of the correct strength and distribution of intrinsic stresses is of great importance for the further considerations within this work. Because here the effect of intrinsic stresses on the resulting stress fields in connection with additional external loads shall be discussed and consequently only the correct assumptions for the intrinsic stresses can guarantee sufficiently correct resulting elastic fields of the combined internal and external loading. For this, however, we would need correct 3-dimensional approaches rather than two dimensional plate approximations as described above.

Thus, we will start with the introduction of linear elastic models providing sufficient flexible tools for the modelling of intrinsic stresses. Because we are interested in the effects of external contact loads, we will concentrate here on intrinsic stress models near surfaces leading us to intrinsic stress profiles of "layered" character. We also need to consider some basics in the modelling of relatively general contact problems. This, however, can be kept short due to the fact that most of the theoretical basics are well published. Applying these modelling tools, we will then consider hypothetical and practical examples demonstrating the importance of intrinsic stresses and their influence on the stability and reliability of mechanically loaded surfaces. By using certain components of the deformation field as critical

values, conclusions can be drawn towards the potential wear behaviour of the material surface in question.

2. Modelling intrinsic stresses

2.1. The simple case of plate-like samples

In those cases where the coating-substrate-compound can be considered as plate-like and the film thickness is small compared to the substrate thickness, the following two assumptions can be made (see for instance [8] or [9]):

- the approximation (1) is valid,
- the film-stress can be considered as being independent from the distance of the interface (here the z-axis shall be parallel to the plate's normal).

This automatically yields a linear z-dependant stress within the substrate [9] and we obtain a very simple stress distribution where only the stress tensor components σ_{xx}, σ_{yy}, $\tau_{xy}=\sigma_{xy}$ are of importance. If we in addition assume to have isotropic or transversely isotropic (the latter with the c-axis parallel to the substrate normal) substrate materials of symmetry of revolution and homogeneous deposition conditions over the whole substrate surface, we result in only one governing stress value σ_{rr}, which is the radial stress[1]. While this stress is widely assumed (e.g. [8]) to be homogeneous within the film, it follows a linear z-dependant function within the substrate. This principle distribution of the σ_{rr} stress component occurs only under the conditions mentioned above.

2.2. A more general three dimensional model for film stresses

Unfortunately for most cases, like coated tools, car components or massive lenses, the assumption of a plate-like film-substrate-compound is not valid and thus the stress distribution might be completely different from that one described above. This holds especially for the substrate. For the film, however, we still can assume that $\sigma_{zz}=0$ is valid and the biaxial stress is homogeneous over the film thickness as long as the film is thin and there is no significant displacement, phase transition or other inelastic effects of any of the parts of the film causing local stress releases. This becomes clear if one notices that the linear z-

---

[1] One can evaluate this by combining the thin plate approximation (1) with the isotropy condition for material properties and deposition process ($\sigma_{xx}=\sigma_{yy}$, $\sigma_{xy}=0$) and the following transformation rules:

$$\sigma_{rr} = \cos^2 \varphi \, \sigma_{xx} + \sin 2\varphi \, \sigma_{xy} + \sin^2 \varphi \, \sigma_{yy} = \sigma_{xx} \, ,$$

$$\sigma_{\varphi\varphi} = \cos^2 \varphi \, \sigma_{yy} - 2 \cos \varphi \sin \varphi \, \sigma_{xy} + \sin^2 \varphi \, \sigma_{xx} = \sigma_{xx} \, ,$$

$$\sigma_{r\varphi} = \cos 2\varphi \, \sigma_{xy} - \sin 2\varphi \, (\sigma_{xx} - \sigma_{yy})/2 = 0 \, ,$$

yielding:

$$\sigma_{ij} = \begin{pmatrix} \sigma_{rr} & 0 & 0 \\ 0 & \sigma_{rr} & 0 \\ 0 & 0 & 0 \end{pmatrix} .$$

dependant stress distribution within the substrate is caused by the bending of the compound but in all cases of non-plate-like substrates this is not possible. So the question arises: If we can still assume a constant σ_{rr}^{f} stress distribution for the coating, how could we come to a suitable stress description for the substrate?

To answer this question we assume the coating to be separated from the substrate and pressed at its rim such that exactly the bi-axial intrinsic stress state with σ_{xx} and σ_{yy} appears. This pre-stressed coating is now "stuck" on the substrate. The external forces Fx and Fy producing the pre-stress-state are removed allowing the coating-substrate-system to find its equilibrium. The former forces acting on the rim of the coating must now be taken on by the elastic stiffness of the substrate. They (the forces) couple into the substrate as shearing forces Sx and Sy via its surface. In order to simplify the calculation, we consider a substrate of square geometry with the side length s. We do not know yet the distribution of this shearing stress on the substrate surface respectively want to keep it as flexible as possible, so we start with a general approach of the problem in the case of a rectangular substrate, which can be given due to the following displacements (variation of the approach given in [10]) $\vec{u} = (u, v, w)$ in x, y and z-direction:

$$
\vec{u} = \sum_{i,k=1}^{\infty} c_{ik}
\begin{pmatrix}
c^2\left((A+Bcz)e^{cz} + (D+Fcz)e^{-cz}\right)\sin[cx] + u^2\left(Ce^{uz} + Ge^{-uz}\right)\cos[uy] \\[2mm]
u^2\left((\tilde{A}+\tilde{B}cz)e^{uz} + (\tilde{D}+\tilde{F}uz)e^{-uz}\right)\sin[uy] + c^2\left(\tilde{C}e^{cz} + \tilde{G}e^{-cz}\right)\cos[cx] \\[2mm]
c^2\left((-A-(-3+4\nu+uz)B)e^{cz} + (D+(3-4\nu+uz)F)e^{-uz}\right)\cos[cx] \\
+ u^2\left((-\tilde{A}-(-3+4\nu+uz)\tilde{B})e^{uz} + (\tilde{D}+(3-4\nu+uz)\tilde{F})e^{-uz}\right)\cos[uy]
\end{pmatrix}
\tag{4}
$$

with $c = \dfrac{i\pi}{a}$, $u = \dfrac{k\pi}{b}$ (a and b denoting the side lengths of the rectangular substrate) and i,k=1,3,5,7…, which assures the normal stresses σ_{xx} and σ_{yy} being zero at the substrate rim. The constants A, B, C, D, F, G and $\tilde{A}, \tilde{B}, \tilde{C}, \tilde{D}, \tilde{F}, \tilde{G}$ are different for each film and substrate; so altogether we have to determine 24 constants in the case of a one-coating-substrate compound. In this case a suitable Fourier series would be necessary to construct the desired stress distribution for either the normal or shearing stresses within any chosen z=constant-plane of the compound. So, for example we could demand $\sigma_{rr}^{f} = \sigma_{\text{intrinsic stress}}^{film}(x, y)$ (e.g. $\sigma_{rr}^{f} = const$) over the whole coating area. It can be shown that (4) satisfies the equation for equilibrium for an isotropic elastic medium. The stress components can be found using the following identities:

$$
\sigma_{jk} = \frac{E}{1+\nu}\left(u_{jk} + \frac{\nu}{1-2\nu}u_{ll}\delta_{jk}\right) \quad with \quad j,k = x, y, z; \ u_{xk} = \frac{\partial u}{\partial k}; \ u_{yk} = \frac{\partial v}{\partial k}; \ u_{zk} = \frac{\partial w}{\partial k}.
\tag{5}
$$

By setting the co-ordinate origin at the interface (z=0), the further boundary conditions:

$$\sigma_{zz}\big|_{z=h_f} = \sigma_{zz}\big|_{z=-h_s} = \sigma_{xz}\big|_{z=-h_s} = \sigma_{yz}\big|_{z=-h_s} = \sigma_{xz}\big|_{z=h_f} = \sigma_{yz}\big|_{z=h_f} = 0,$$

$$\sigma_{xz}\big|_{z=0+0} = \sigma_{xz}\big|_{z=0-0} = f_x(x,y),\ \sigma_{yz}\big|_{z=0+0} = \sigma_{yz}\big|_{z=0-0} = f_y(x,y),$$

$$\sigma_{zz}\big|_{z=0+0} = \sigma_{zz}\big|_{z=0-0},\quad u_3\big|_{z=0+0} = u_3\big|_{z=0-0},$$

$$Fx = \sigma_{rr}^f h_f b = Sx = \int\limits_{-b/2}^{b/2}\int\limits_{0}^{a/2} \sigma_{xz}\,dx\,dy,$$

$$Fy = \sigma_{rr}^f h_f a = Sy = \int\limits_{-a/2}^{a/2}\int\limits_{0}^{b/2} \sigma_{yz}\,dy\,dx.$$

give the equations necessary to determine all constants. One can extract from (4) that the structure of the normal stresses in lateral direction of the film-substrate-compound σ_{xx} and σ_{yy} can in principle be given in the following form:

$$\sigma_{xx} = \sum_{i=1}^{\infty} fx_x(z)\,c_i \cos\left(\frac{i\pi x}{a}\right) + \sum_{k=1}^{\infty} fx_y(z)\,c_k \cos\left(\frac{k\pi y}{b}\right),$$

$$\sigma_{xx} = \sum_{i=1}^{\infty} fy_x(z)\,c_i \cos\left(\frac{i\pi x}{a}\right) + \sum_{k=1}^{\infty} fy_y(z)\,c_k \cos\left(\frac{k\pi y}{b}\right).$$

(6)

Now we need to find equations for the determination of the Fourier coefficients c_i and c_k. From the bi-axial stress conditions $\sigma_{xx}^f = \sigma_{yy}^f = \sigma$ =const at a distinct depth $z=z_0$ together with (6), we obtain:

$$c_i = \frac{2}{a}\int\limits_{-a/2}^{a/2} \frac{\sigma\left(fx_y(z_0) - fy_y(z_0)\right)}{fx_y(z_0)\,fy_x(z_0) - fx_x(z_0)\,fy_y(z_0)} \cos\left(\frac{i\pi x}{a}\right),$$

$$c_k = \frac{2}{b}\int\limits_{-b/2}^{b/2} \frac{\sigma\left(fx_y(z_0) - fy_y(z_0)\right)}{fx_y(z_0)\,fy_x(z_0) - fx_x(z_0)\,fy_y(z_0)} \cos\left(\frac{k\pi y}{b}\right).$$

(7)

In the case of a square sample of side length s the equations above simplify significantly:

$$\vec{u} = \sum_{\forall i,k} c_{ik}
\begin{pmatrix}
au\left((A+B+Buz)e^{uz} - (D-F+Fuz)e^{-uz}\right)Sx*\sin[ax] \\
bu\left((A+B+Buz)e^{uz} - (D-F+Fuz)e^{-uz}\right)Sy*\sin[by] \\
u^2\begin{pmatrix}(-A+(2-4v-uz)B)e^{uz} \\ -(D+(2-4v+uz)F)e^{-uz}\end{pmatrix}(Sx*\cos[ax] + Sy*\cos[by])
\end{pmatrix}$$

(8)

with u=a=b and $a = \dfrac{i\pi}{s},\quad b = \dfrac{k\pi}{s}$ and i,k=1,3,5,7…, which again assures the normal stresses σ_{xx} and σ_{yy} being zero at the substrate edges when the co-ordinate origin is laid in the centre of the rectangle's surface. The further boundary conditions at the interface, surface and bottom must now read:

$$\sigma_{zz}\big|_{z=0} = \sigma_{zz}\big|_{z=h_s} = \sigma_{xz}\big|_{z=h_s} = \sigma_{yz}\big|_{z=h_s} = 0,\quad \sigma_{xz}\big|_{z=h_s} = \sigma_{yz}\big|_{z=h_s} = f(x,y),$$

$$Fx = Fy = \sigma_{rr}^f hs = Sx = Sy = \int\limits_{-s/2}^{s/2}\int\limits_{0}^{s/2} \sigma_{xz}\,dx\,dy = \int\limits_{-s/2}^{s/2}\int\limits_{0}^{s/2} \sigma_{yz}\,dy\,dx$$

They give the equations necessary to determine all constants including the coefficients c_{ik}.

N. Schwarzer, About Intrinsic Stresses – their effects and measurement via indenter, publication of the Saxonian Institute of Surface Mechanics, online at www.siomec.de/pub/2007/001

contact@siomec.de   www.siomec.de

5

In the case of thin films and plate-like substrates this approach should agree with the results given by the equation of Stoney, which in fact it does [9, 11].

It should be pointed out here that by extending the method described above to several layers with more degrees of freedom for defining arbitrary stress distributions at a multitude of planes in z-direction, also relatively complex intrinsic stress distributions can be constructed.

2.3. A defect model: Tool for the construction of relatively general intrinsic stress distributions

Introducing circular defects of radii a_i of the loading type:

$$\tau_{rz0}(r_i = \sqrt{(x-x_i)^2+(y-y_i)^2}, z_i+0) = \sum_{n=0}^{N} c_{\tau i,n} r_i^n \sqrt{a_i^2 - r_i^2}$$
$$\tau_{rz0}(r_i = \sqrt{(x-x_i)^2+(y-y_i)^2}, z_i-0) = -\sum_{n=0}^{N} c_{\tau i,n} r_i^n \sqrt{a_i^2 - r_i^2}$$
(9)

$$\sigma_{zz0}(r_i = \sqrt{(x-x_i)^2+(y-y_i)^2}, z_i+0) = \sum_{n=0}^{N} c_{\sigma i,n} r_i^n \sqrt{a_i^2 - r_i^2}$$
$$\sigma_{zz0}(r_i = \sqrt{(x-x_i)^2+(y-y_i)^2}, z_i-0) = -\sum_{n=0}^{N} c_{\sigma i,n} r_i^n \sqrt{a_i^2 - r_i^2}$$
(10)

(with x_i, y_i, z_i denoting the centre of the defect and n=0,2,4,6) directly allows us the application of the extended Hertzian approach [12] that provides a complete solution of the elastic field of the defect loading given above. By superposing a multitude of such "defect dots" one could model (simulate) a very great variety of intrinsic stress distributions. The evaluation of the complete elastic field is straight forward. It only requires the evaluation of certain derivatives of the potential functions given in [12].

3. Modelling of contact loads for layered materials

3.1. A brief description of the extended Hertzian approach

It is well known that the classical Hertzian theory [13] describes the normal surface displacements of parabolically shaped indenter (with displacement w_I) and sample body (with displacement w_S) of similar geometry due to:

$$w_S(r) + w_I(r) = h - \frac{r^2}{d_0},$$
(11)

(r is giving the distance to the contact centre and d_0 is a parameter depending on the radii of curvature of both indenter and sample-body). Because this theory does not provide enough degrees of freedom for the modelling of more practical contact problems, Schwarzer extended the Hertzian theory [12] and evaluated the complete potentials necessary to obtain the elastic field for a governing contact equation of the type

$$w_S(r) + w_I(r) = h - \frac{r^2}{d_0} - \frac{r^4}{d_2} - \frac{r^6}{d_4} - \frac{r^8}{d_6}.$$
(12)

N. Schwarzer, About Intrinsic Stresses – their effects and measurement via indenter, publication of the Saxonian Institute of Surface Mechanics, online at www.siomec.de/pub/2007/001
contact@siomec.de   www.siomec.de

6

He also presented the procedures necessary to obtain the potential functions for even higher exponents n of r^n. Thus, now normal and even tangential [14] load distributions of the form

$$\sigma_{zz0}(r,\varphi) = \sum_{n=0}^{N} c_{\sigma n} r^n \sqrt{a^2 - r^2} \tag{13}$$

$$\tau_{rz0}(r,\varphi) = \sum_{n=0}^{N} c_{\tau rn} r^n \sqrt{a^2 - r^2}$$

$$\tau_{xz0}(r,\varphi) = \sum_{n=0}^{N} c_{\tau xn} r^n \sqrt{a^2 - r^2} \tag{14}$$

$$\tau_{yz0}(r,\varphi) = \sum_{n=0}^{N} c_{\tau yn} r^n \sqrt{a^2 - r^2}$$

with n=0,2,4,6 and arbitrary constants c (and by following the instructions of the mathematical procedures for obtaining the complete potential functions as given in [12] and [14] even arbitrary high but only even N) can be solved completely.
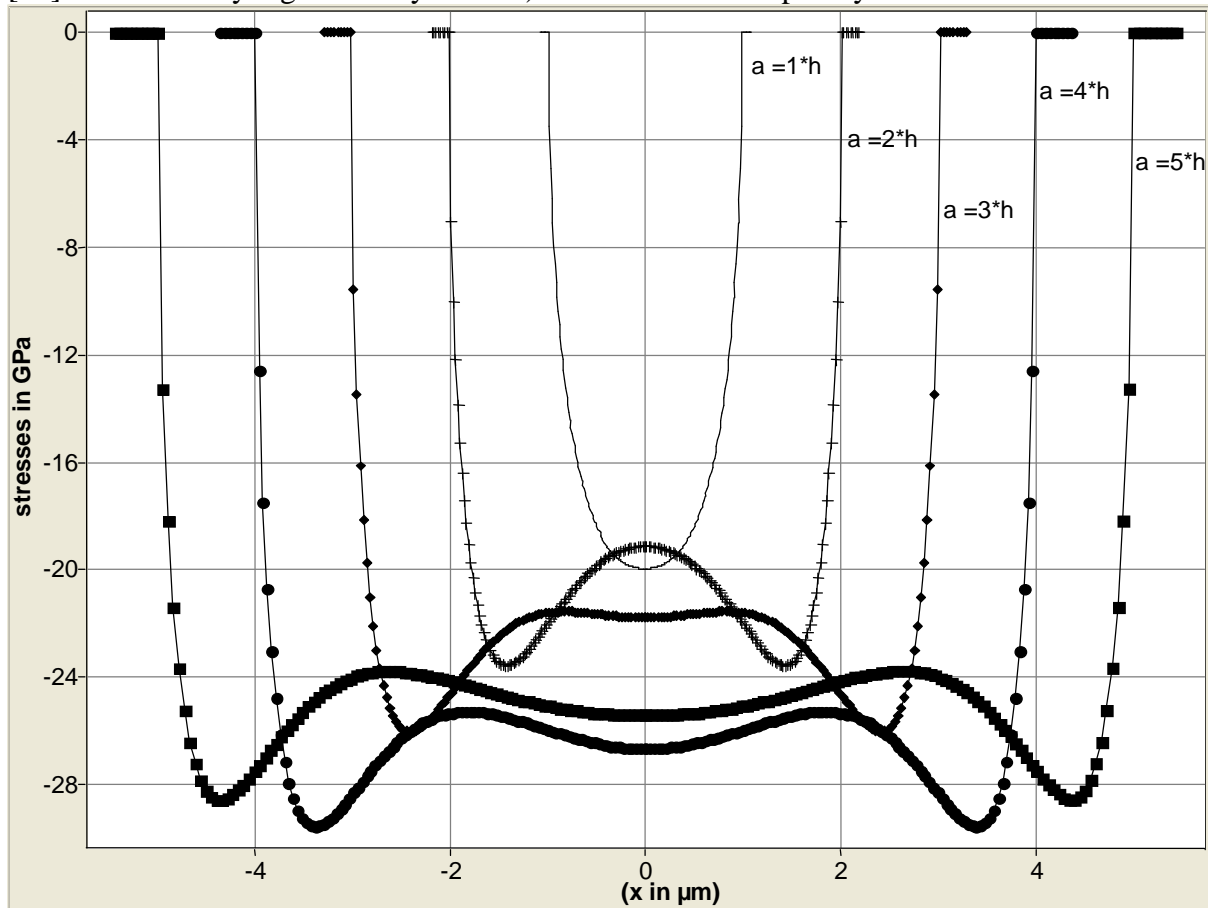

Fig. 1:   Resulting normal pressure distribution for a variety of ratios of contact radius a (= 1µm to 5µm) to coating thickness h=1µm evaluated for a coating substrate-compound with equal Poisson's ratios and Young's moduli 700GPa (coating) on 70GPa. Radius of indenter: 10µm (diamond). Evaluation performed with the software FilmDoctor [23] using the extended Hertzian approach.

Together with the lateral load one often faces tilting moments leading to a normal surface stress distribution of the form

$$\sigma_{zz0}(r,\varphi) = \sum_{n=0}^{N} c_{\sigma n} r^{n+1} \cos(\varphi) \sqrt{a^2 - r^2} \ . \qquad (15)$$

These stresses can for example occur when the indenter shaft is dragged over the surface. Because the shaft itself is elastic and thus would be bent during the lateral loading, an unavoidable tilting moment results on the contact surface. Also curved surfaces (e.g. due to roughness) can lead to such tilting moments.

This opens up a wide range of new analysing techniques in order to extract more information from indentation experiments [12-16] even in cases of very thin coatings below 100nm [17] where the approach has been used to extract the yield strength of coatings down to 35nm. Motivated by the structures of the new governing contact equation (12), this approach has been dubbed "extended Hertzian" by the author.

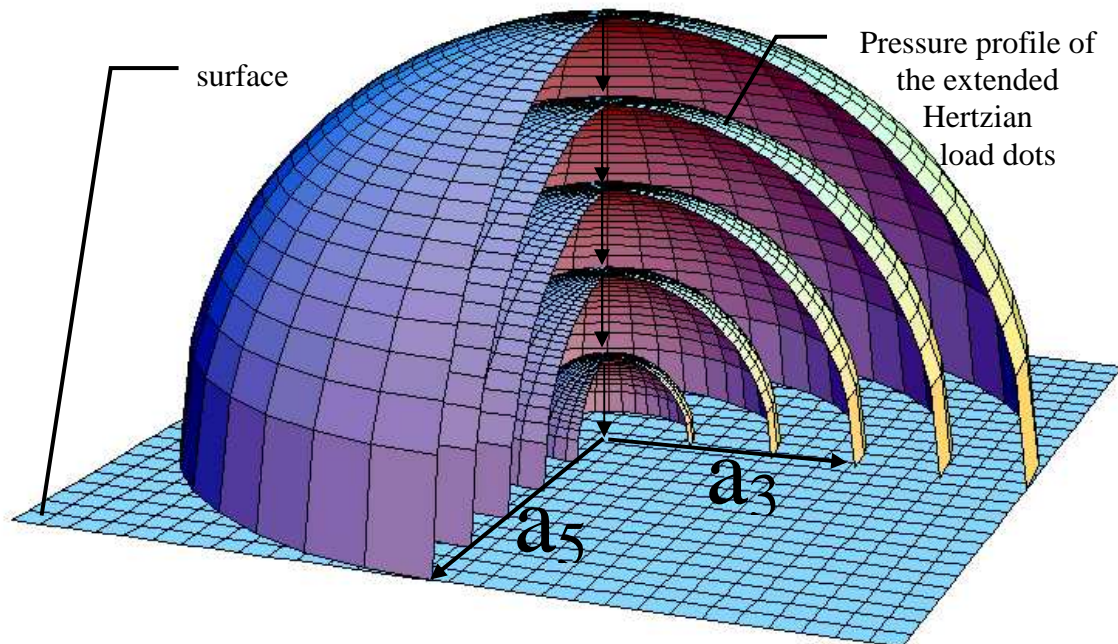The approach and its uses have been considered rather comprehensively in [18].

Fig. 2: Illustration of the mathematical method of superposition of extended Hertzian load distributions with different contact radii a_i (and in principle also different loads).

3.2. Extension to layered materials

By applying the method of image loads, the approach given above can also be extended to layered materials [19]. This is of special importance for all sorts of mechanical contact problems of symmetry of revolution if one intends to determine the resulting normal stress distribution which can be quite different from the non layered case (fig. 1). With a special mathematical procedure [11] the method of image loads can also be used for the modelling of graded coatings.

3.3. Extension to load-dots

Another useful extension is the introduction of several load dots [11] allowing to treating of even more complex contact problems (fig. 2). This method can for example be used to

N. Schwarzer, About Intrinsic Stresses – their effects and measurement via indenter, publication 8
of the Saxonian Institute of Surface Mechanics, online at www.siomec.de/pub/2007/001
contact@siomec.de   www.siomec.de

incorporate the otherwise neglected lateral displacement [20] for a more accurate treatment of e.g. indentations with conical indenters [21] or to correctly describe the tip rounding of indenters during depth sensing indentation experiments (examples are to be found in [17] and fig. 3 → in the latter both tip rounding and the effect of lateral displacement has been taken into account) or – as done in section 6 of this paper – to superpose distinct normal and lateral loads in order to simulate a spherical or conical punch in parts bonded to the sample.
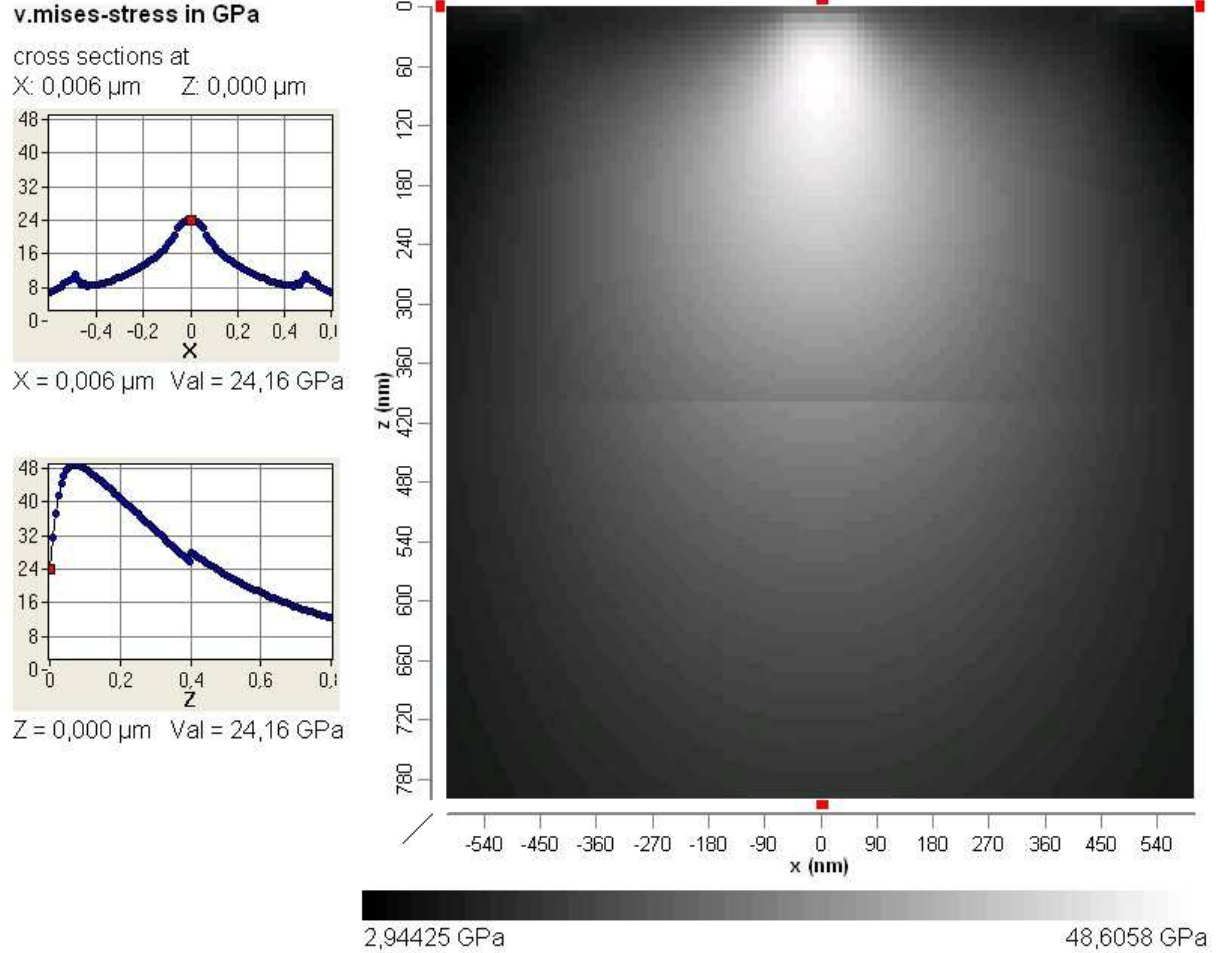

Fig. 3: **Resulting von Mises stress distribution for a diamond cone (half angle 70.3°) with rounded tip (radius of tip 190nm) pressed into a CN$_x$-coating of 400nm thickness with 130GPa Young's modulus (Poisson's ratio 0.25) on silicon at 20mN. The evaluation has been performed with the software FilmDoctor [23] using a load dot model with 30 load dots (c.f. fig. 2).**

3.4. Extension to rotating indenters

Another useful tool might be the model of a rotating indenter, because here one could combine the advantage of adding a shearing load component with maintaining the symmetry of revolution. In order to model this type of mixed loading, one simply has to add the following shearing stress distribution

$$\tau_{xz0}(r,\varphi) = -\sum_{n=0}^{N} c_{ROT\,n} r^{n+1} \sin(\varphi)\sqrt{a^2 - r^2}$$

$$\tau_{yz0}(r,\varphi) = \sum_{n=0}^{N} c_{ROT\,n} r^{n+1} \cos(\varphi)\sqrt{a^2 - r^2}$$

(16)

to the normal load on the surface of the sample.

N. Schwarzer, About Intrinsic Stresses – their effects and measurement via indenter, publication   9
of the Saxonian Institute of Surface Mechanics, online at www.siomec.de/pub/2007/001
contact@siomec.de   www.siomec.de

4. Evaluation

The potential functions necessary for the evaluation of the elastic fields of the above given surface load distributions can be evaluated by applying the method of Fabrikant [22]. The method can be applied directly for homogeneous half spaces and in combination with the image load method [19] also for layered materials. However, all of the models mentioned above are woven into a software package [23] which can be considered as a tool box for modelling a great variety of internal and external load problems for homogeneous and layered materials. The package can be downloaded and used for free for a restricted time. Some models and features are also accessible for free via an internet portal (www.siomec.de/service) without the need of downloading or installing special technical software. Within this paper we will rather often use the von Mises stress given as

$$\sigma_M = \sqrt{\frac{1}{2}\left(\left(\sigma_{xx}-\sigma_{yy}\right)^2+\left(\sigma_{zz}-\sigma_{yy}\right)^2+\left(\sigma_{xx}-\sigma_{zz}\right)^2+6*\left(\tau_{xy}^2+\tau_{xz}^2+\tau_{zy}^2\right)\right)}.$$
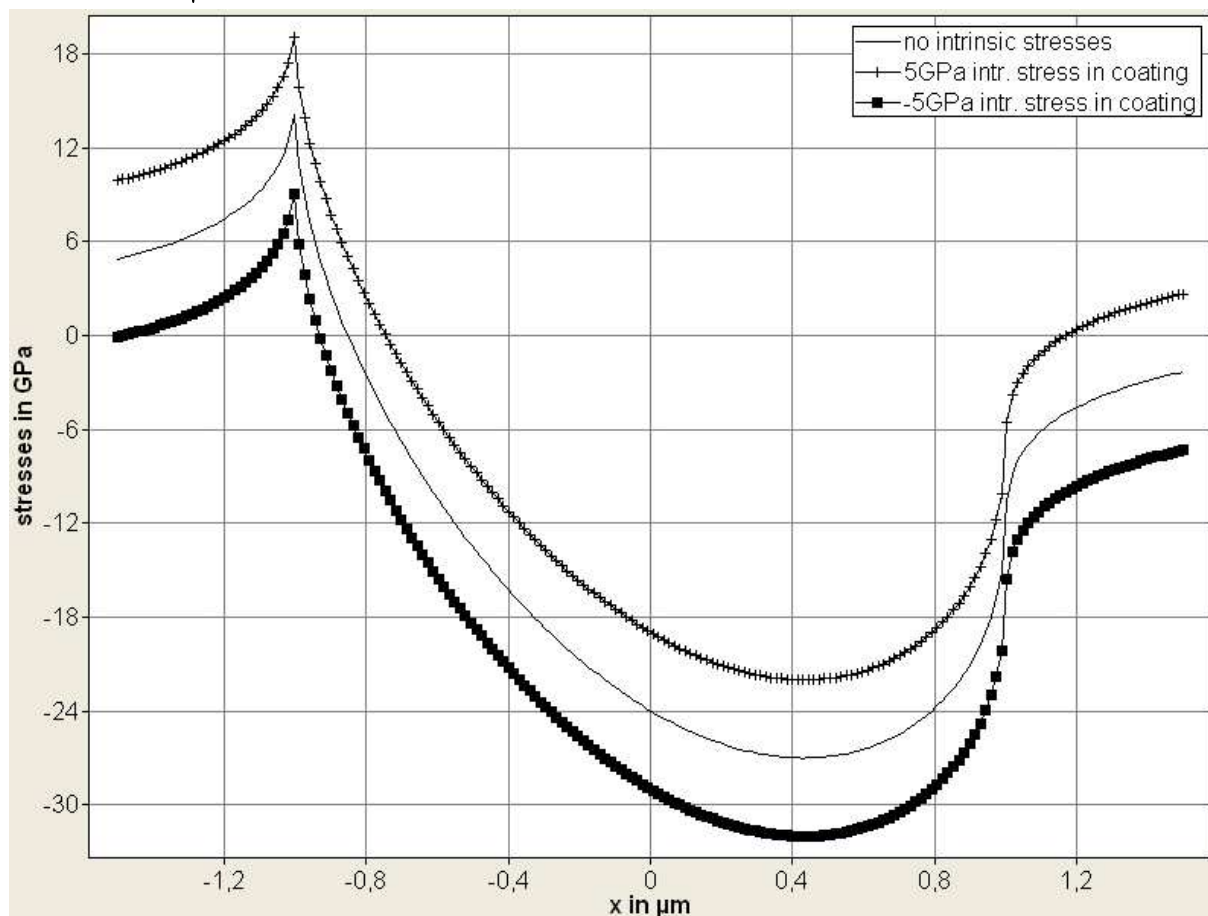

Fig. 4: **Resulting normal stress in x-direction for a single-layer substrate system with mixed normal and lateral load (load 52.7mN, sliding friction with μ=0.3, contact radius 1μm; material parameters given in section 5.2) for different intrinsic coating stresses.**

5. About the effect of intrinsic stresses on the load carrying capacity of homogeneous and layered materials

The basis of the following considerations is the assumption that mechanical wear starts with failures caused by certain stress fields exceeding critical limits at distinct points or areas within the material. Due to effects like defect accumulation or propagation it might well be that only repeated loading respectively exceeding of these critical stress values results in

failure. This, however, does not compromise our view that a great variety of nanoscopic mechanical failure and subsequent wear can be described as a function of certain critical stress values perhaps together with also critical numbers of load cycles where such critical stresses occur. The stress fields are either caused by external or internal (intrinsic) loads. Here we will mainly consider biaxial intrinsic stress distributions, e.g. stresses laying in-plane and parallel to the surface. Assuming now that surface fracture is caused by tensile stresses, one can easily deduce that the biaxial intrinsic stresses linearly increase or decrease the probability for such failure. This is because stresses in the linear elastic regime are simply additive and so the biaxial stress must be added to the stresses resulting from any external load. Thus, one finds decreasing mode I surface fracture probability for compressive, and increasing probability for tensile biaxial intrinsic stresses. We demonstrate this for a simple one-layer-substrate system with Hertzian load and additional lateral surface traction in x-direction (scratch with Coulomb friction µ=0.3, see figure 4). However, for other failure mechanisms like mode II, mode III fracture and plastic flow no such simple answers can be given because the combination of intrinsic and external loads often results in relatively complex stress distributions. Here a stringent and comprehensive consideration of the resulting deformation fields is necessary in order to decide upon the load carrying capacity of the material in question with respect to a certain loading situation.

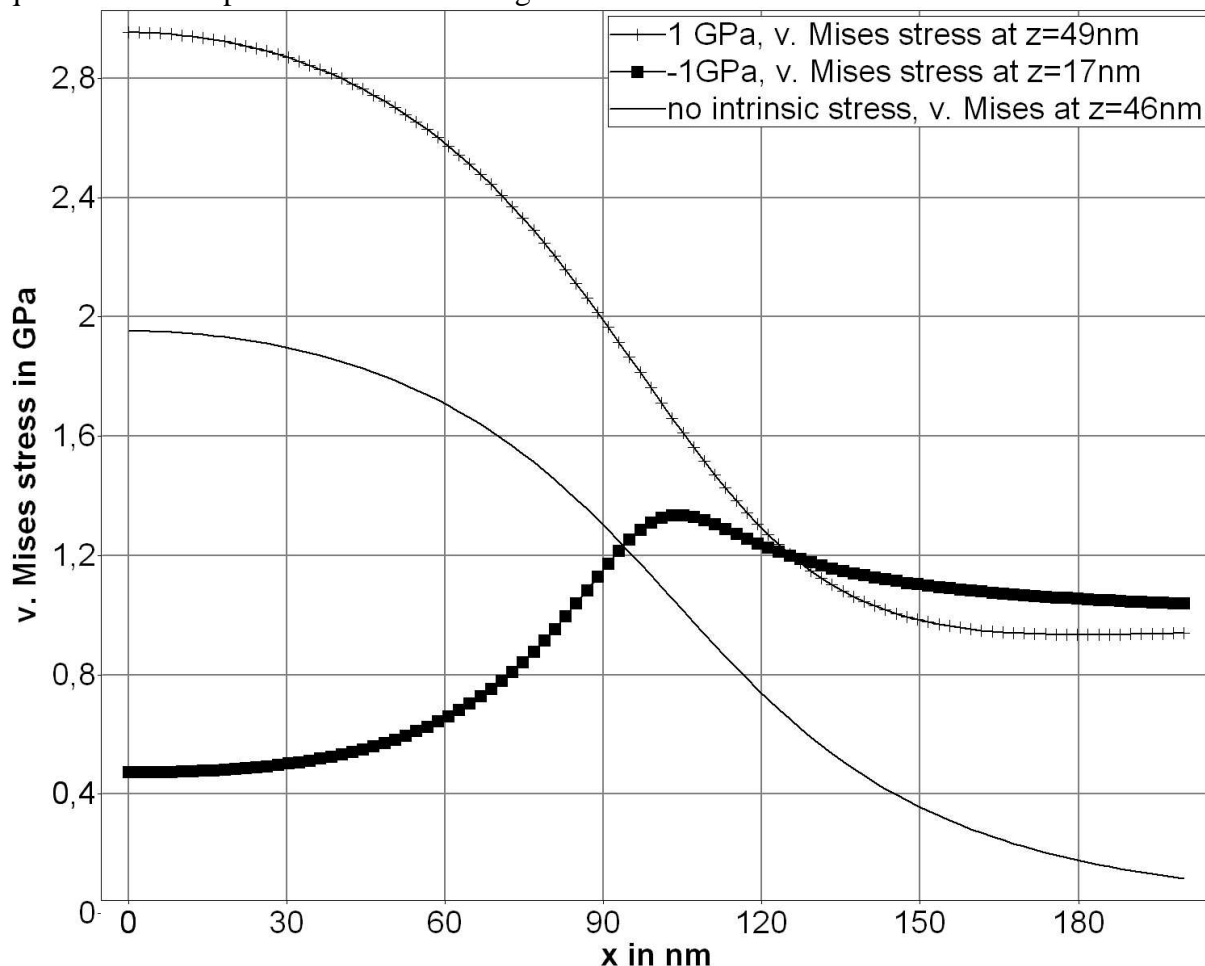**Fig. 5:** **Resulting von Mises stress for a homogeneous material (steel) with pure Hertzian normal load (load 66µN, contact radius 0.1µm) for different exponentially decreasing intrinsic stresses as given in section 5.1 with C_0=1 and σ_0 given in the legend.**

5.1. Homogenous half spaces

We assume an intrinsic stress distribution of the form

$$\sigma_{xx}^I = \sigma_{yy}^I = \sigma_0 \, e^{-C_0 z},$$

which could for example occur when a mechanical surface treatment has been applied to a rim hardened steel sample. We investigate the resulting load carrying capacity with respect to plastic flow with a yield strength of 3GPa for the unstressed material. Fig. 5 shows that tensile stresses only increase the von Mises stress without significant changes of the stress distribution, meaning we still would find the von Mises Maximum along the axis of indentation. However, compressive biaxial intrinsic stresses, apart from decreasing the von Mises stresses, lead to a completely different picture. In fig. 5 the von Mises stress for the compressive intrinsic case was thus drawn along the x axis at z=16nm where we found the maximum, while this maximum for the unstressed and the tensile intrinsic stress case was to be found much deeper underneath the contact zone. Here, for tensile and no intrinsic stresses, always an ellipsoid-like plastic zone would be formed while in the compressive case the von Mises maximum is to be found within a torus-like region beneath the contact surface resulting in a topologically completely different plastic zone if the yield strength would be exceeded. We will investigate this topologic development in more detail for layered materials in the next section.
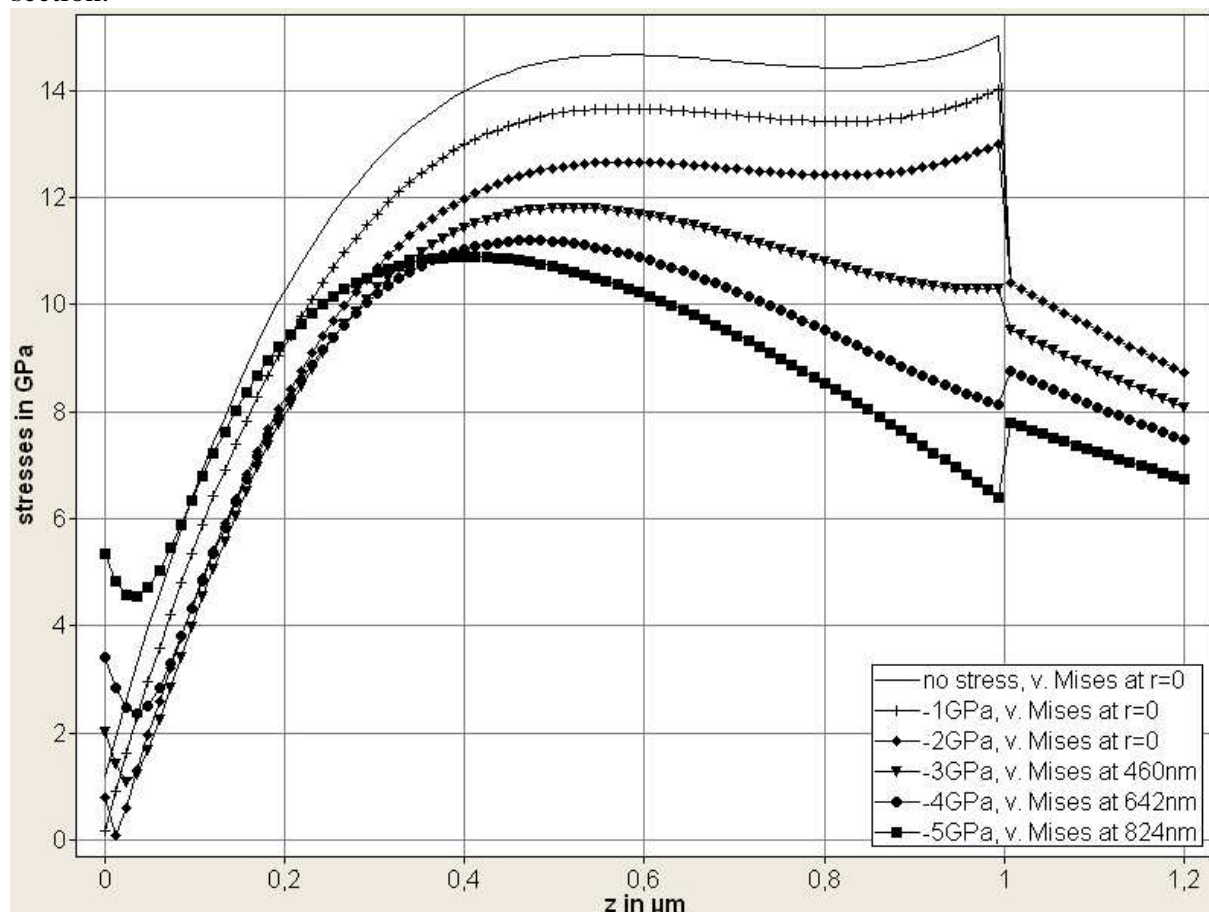

Fig. 6: **Resulting von Mises stress distribution for pure normal loaded (52.7mN) bi-axially stressed coatings with different compressive coating stresses (material parameters are given in section 5.2). The stresses are always drawn at the lateral position of the maximum.**

5.2. Layered half spaces with monolithic layers

We now want to investigate the effect of increasing compressive stresses on the resulting von Mises stress distribution for a single layer 1µm-hard-coating-substrate system with 450GPa Young's modulus for the coating (Poisson's ratio 0.25) and 220GPa for the steel substrate (Poisson's ratio 0.3). We find (fig. 6) that with an increasing compressive and homogeneously distributed biaxial coating stress the von Mises maximum "wanders" from the symmetry axis at the interface within the hard coating towards the surface near the contact rim (fig. 7). We also find that the von Mises maximum decreases with increasing compressive coating stresses. This might lead us to the conclusion that compressive coating stresses are a good thing if it comes to protect coatings from plastic flow. Yes, but we have to be cautious here when we deal with mixed loading conditions, because in that case the compressive stresses might not be as "helpful" as they appear to be in the pure normal loading state (fig. 8). For relatively high friction coefficients or sticking contact situations namely, the von Mises maximum appears on the surface and here (under the same contact loading condition – c.f. fig. 8) the stress in the compressively stressed coating might even exceed its limit of stability (yield strength) earlier than the coating with no intrinsic stress. This means however, that finding high hardness (respectively yield strength) with the classical nanoindenter (pure normal load) does not automatically mean that this high hardness (yield strength) does apply to all loading conditions, because the apparently high hardness value might just be the result of rather high compressive intrinsic stresses. This is of special importance when lifetime predictions, stability limits and the behaviour with respect to mechanical wear shall be extracted from indentation experiments. Then the intrinsic stress should be known and taken into account with respect to the expected loading conditions of the later application in question.
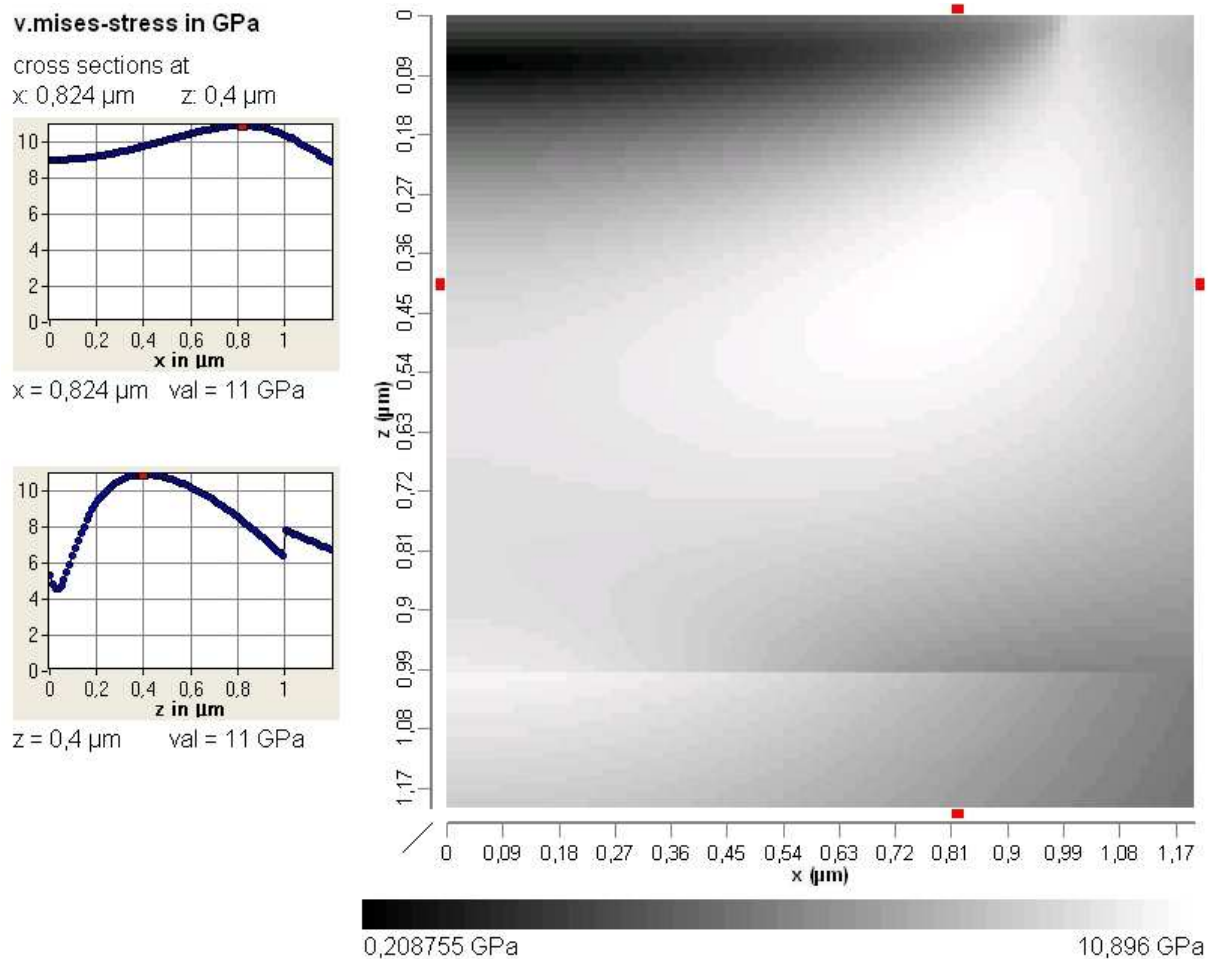
Fig. 7: **Resulting von Mises stress distribution for pure normal loaded (52.7mN) bi-axially stressed coatings with –5GPa compressive coating stresses (material parameters are given in section 5.2).**

5.3. Layered half spaces with graded coatings

There exist quite a variety of recently published papers (e.g. [24]) suggesting the use of functionally graded coatings in order to improve their reliability and load carrying capacity. Here we want to investigate their behaviour under the existence of intrinsic stresses. As example we consider the "optimum" design proposed in [24] with a Young's modulus shape perfectly fitting to the substrate, increasing towards the surface, reaching a plateau and then decreasing again in order to reduce tensile surface stresses. Even though one might argue that for most practical graded coating systems (e.g. [25]) the intrinsic stress would change with the Young's modulus due to their connection within the deposition process, we here assume constant intrinsic coating stresses in order to allow comparison with the monolithic coatings considered in the section above. However, with the software system [23] such intrinsic stress distributions can be modelled easily together with the functionally graded coatings. Here the function for the Young's modulus profile can be given as

$$E(z) = -(z-0.3\mu m)^2\, 469GPa/1\mu m + 450GPa.$$

The result is shown in figure 9. We do not only find that the gradient coating without intrinsic stress reaches a higher von Mises stress maximum than a homogeneous 450GPa-coating would reach at the same load, but that the development of a torus-like von Mises maximum region starts at much higher compressive coating stresses. Thus, we see that the knowledge of the real structure - monolithic, abrupt layered or graded - of a given coating system is of great importance for the discussion of the influence of intrinsic stresses and external loads.
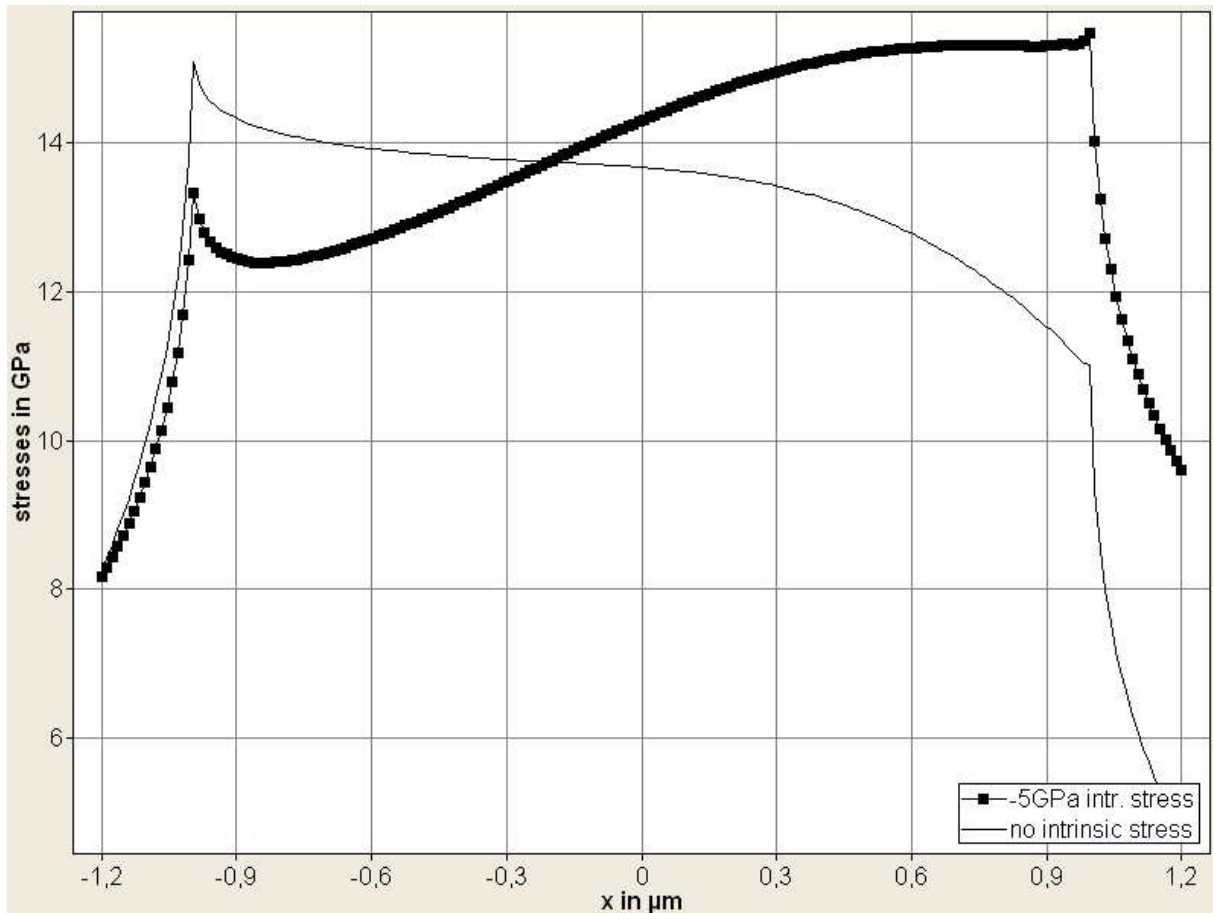
Fig. 8: Resulting von Mises stress distribution for mixed normal (33mN) and lateral load (µ=0.5) on the coating system given in section 5.2 for no intrinsic stress and biaxial compressive coating stress of –5GPa.

5.4. About the modelling-potentials of certain defects

With the introduction of a "defect model" of the type given in section 2.3, the variety of accessible intrinsic stress distributions is infinite and cannot be comprehensively discussed within this paper. It should be mentioned, however, that by superposing such defects in great number and in distinct patterns beneath the surface of our material of interest, effects like surface treatment and residual plastic stresses or any other intrinsic stress distributions being residuals from former loading situations could be taken into account. As an example we restrict ourselves here to the consideration of the use of "shear-load-defect-models" at the interface between coating and substrate. We assume that a defect of the loading form given in (9) is caused by a mismatch of the thermal expansion coefficient between coating and substrate and that the defect is used as modelling tool in order to provide constant normal lateral stresses within the coating. We find a relatively good simulation with the following set of constants for the loading approach (9):

$$c_{\tau i,0} = 1, \quad c_{\tau i,2} = 0.5014 * a^{-2}, \quad c_{\tau i,4} = 0.3452 * a^{-4}, \quad c_{\tau i,6} = 0.4957 * a^{-6}.$$

By choosing a sufficiently big defect radius "a", the area of almost constant lateral normal stress can be made as big as possible. So would for example our 1µm-450GPa-steel-system require a defect radius a of 100µm in order to find rather homogenous lateral normal stresses within a radius of about 70µm. For higher accuracy or special intrinsic stress distributions simply more of such defects have to be superposed. This superposition can also lead to interlinking defect areas as shown in figure 2, where it was used for a special surface stress distribution.
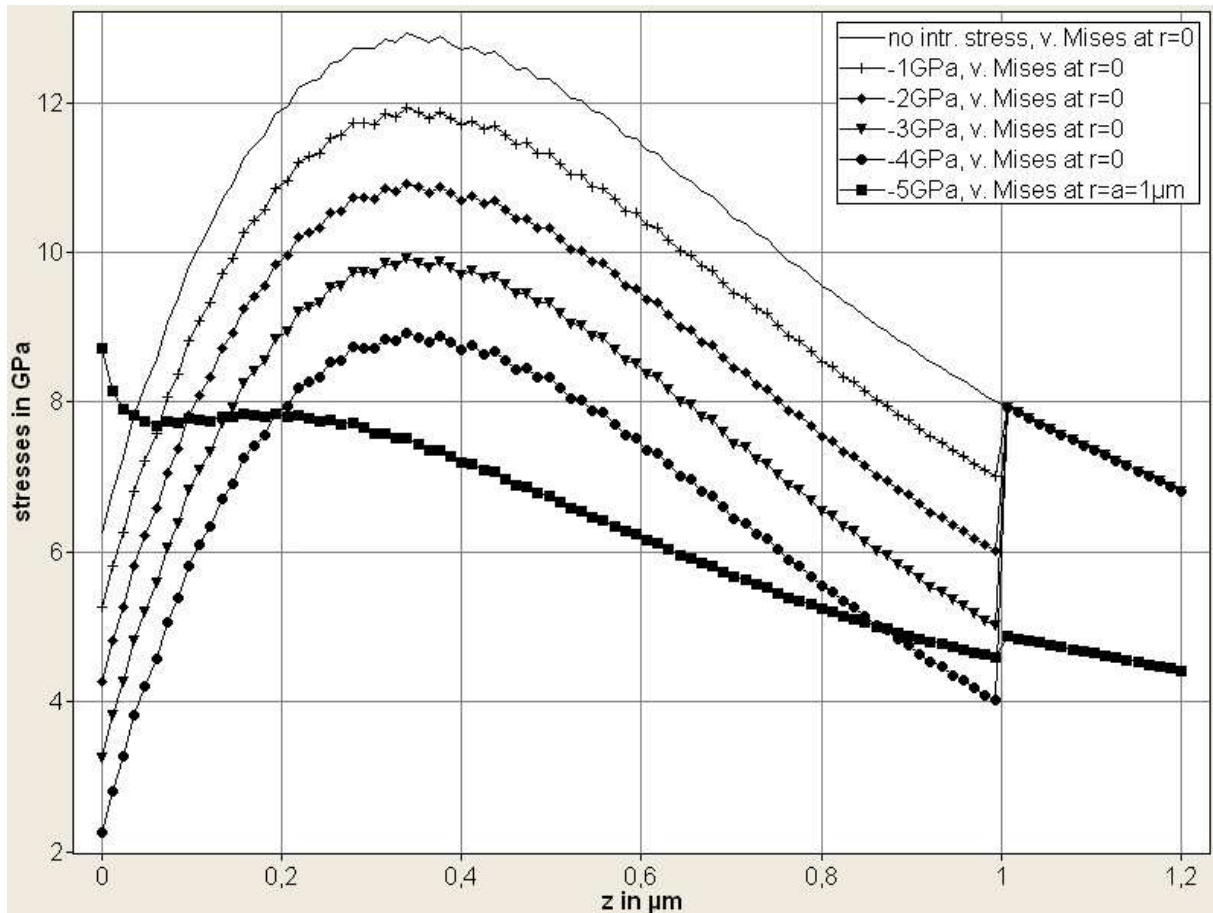
Fig. 9: Resulting von Mises stress distribution for pure normal loaded (52.7mN) bi-axially stressed gradient coatings with different compressive coating stresses (material parameters are given in section 5.3). The stresses are always drawn at the lateral position of the maximum.

6. *Hypothetical method of determining intrinsic stresses in layered materials via nanoindentation*

The problem of measuring intrinsic stresses in monolithic materials using nanoindentation techniques has been proved experimentally possible by Swadener et al [26] and Taljat and Pharr [27]. Some experimental results concerning the immense influence of the intrinsic film stresses on the measured indentation hardness have been published by Coronal et al [28]. Using finite element modelling, Anantha Ram et al [29] have evaluated the Young's modulus and the residual stresses from nanoindentation experiments. Here we discuss the possible application of this method on the measurement of intrinsic thin-film-stresses using the analytical analysing techniques introduced above.

N. Schwarzer, About Intrinsic Stresses – their effects and measurement via indenter, publication 16 of the Saxonian Institute of Surface Mechanics, online at www.siomec.de/pub/2007/001

contact@siomec.de   www.siomec.de
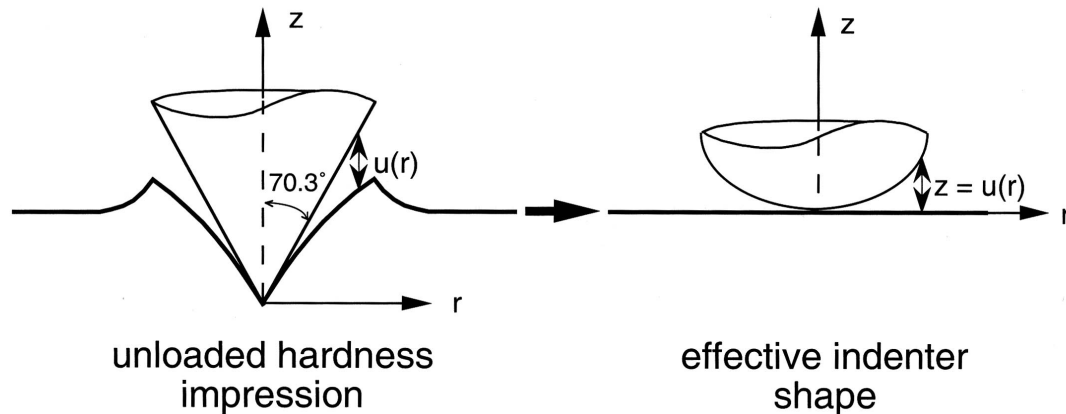
Fig. 10: Schematic presentation of Pharr's concept of the effectively shaped indenter.

6.1. Applying pure normal and mixed normal-lateral loads with sharp indenters

In [11], Schwarzer has considered a variety of methods to determine intrinsic film stresses by means of spherical indenters. However, the main disadvantage of the methods dependent on spherical or other blunt indenters as described there is the necessity of determining the yield strength within a cyclic loading unloading procedure with well defined blunt indenters. This increases the error liability of the method. Desirable would be a method allowing the determination of this parameter within "one go", meaning that only one cycle of penetration would suffice in order to obtain a proper value for either the yield strength or other limiting mechanical parameters. Such a method is already at hand. It is called the "concept of the effectively shaped indenter" and has been introduced in the form used here by G. M. Pharr some years ago (see e.g. [30]). Using an extended Hertzian approach [12], the author has been able to apply this method to monolithic, single layer and even functionally-graded coated materials (see also [14 - 17] and [25, 31]). As the method is extensively described in the four papers mentioned above, only a very brief description shall be given here.

We assume an otherwise arbitrarily shaped sharp indenter (Vickers, Berkowich, etc.) being pressed into a layered material producing an elastic-plastic state of deformation (fig. 10, left part). It is known that in quite a lot of cases - after a sufficient holding time - the unloading process starts completely elastically. The basic idea behind "the concept of the effectively shaped indenter" is to find a blunt indenter of symmetry of revolution which would produce the same unloading curve as the original sharp indenter does in the beginning of the unloading process. This is done by making use of a "quasi conform geometrical transformation" of the surfaces of sample and indenter. This way the otherwise very cumbersome boundary conditions of the purely elastic unloading process directly after the indenter has reached its maximum depth can dramatically be simplified. The reason is the substitution of the problem of a well defined indenter acting on a pre-deformed surface by the problem of an effectively shaped indenter and a flat surface (fig. 10, right part). This allows a better discussion of the load-displacement curve in connection with the effects occurring during the penetration process.

Now we propose the following measuring procedure:

1. The yield strength is determined using the method of the effectively shaped indenter as presented above. However, during unloading, the indenter is only drawn back to a distinct fraction of the maximum load p_0. This load shall be called p_1. The reader should note that p_1

N. Schwarzer, About Intrinsic Stresses – their effects and measurement via indenter, publication 17 of the Saxonian Institute of Surface Mechanics, online at www.siomec.de/pub/2007/001

contact@siomec.de   www.siomec.de

must be chosen such that on the one hand there is "enough unloading curve" for the determination of the shape of the effective indenter, and on the other hand the load is still big enough in order to avoid strong and dominant inelastic unloading effects like e.g. unloading fractures. In addition, a p_1 close to p_0 also assures that the shape of the effective indenter only changes in an insignificant manner during unloading. We call the determined yield strength σ_M^{crit}. Here we now have to add the two elastic fields resulting from the intrinsic stresses σ_{ij}^I and the nanoindenter loading σ_{ij}^L. The von Mises stress can be written in the following form:

$$\sigma_M = \sqrt{\frac{1}{2}\left(\left(\sigma_{xx}-\sigma_{yy}\right)^2+\left(\sigma_{zz}-\sigma_{yy}\right)^2+\left(\sigma_{xx}-\sigma_{zz}\right)^2+6*\left(\tau_{xy}^2+\tau_{xz}^2+\tau_{zy}^2\right)\right)}$$

with $\sigma_{ij}=\sigma_{ij}^I+\sigma_{ij}^L$.

2. Now a slowly oscillating tangential load component t_x with increasing amplitude is added and the resulting lateral shift is measured. So we now have mixed load conditions and assume our - in step one determined - effectively shaped indenter acting with the combined load components p_1 and t_x onto the coating substrate compound.

3. The slowly oscillating tangential loading with increasing amplitude is monitored with very high resolution (as well as the static normal load and displacement, of course) until nonlinear behavior can be detected. Thus, the value of maximum tangential load $t_x=t_{crit}$ or maximum lateral displacement u_σ is determined. Now we introduce the following assumption: The combined stresses add up to a mechanical stress field producing a maximum von Mises stress $\sigma_M=\sigma_M^{crit}$ somewhere within the investigated coating material.

4. With these two measurements and the resulting measured values p_0, p_1, the corresponding penetration depth, t_{crit} and u_σ we can construct two linear independent equations

$$\sigma_M^{crit} = \sqrt{\frac{1}{2}\left(\begin{array}{l}\left(\sigma_{xx}^L-\sigma_{yy}^L+\sigma_{rr}^f\left(f_{xx}^I-f_{yy}^I\right)\right)^2+\left(\sigma_{zz}^L-\sigma_{yy}^L+\sigma_{rr}^f\left(f_{zz}^I-f_{yy}^I\right)\right)^2 \\ +\left(\sigma_{xx}^L-\sigma_{zz}^L+\sigma_{rr}^f\left(f_{xx}^I-f_{zz}^I\right)\right)^2 \\ +6*\left((\tau_{xy}^L+\sigma_{rr}^f f_{xy}^I)^2+(\tau_{xz}^L+\sigma_{rr}^f f_{xz}^I)^2+(\tau_{zy}^L+\sigma_{rr}^f f_{zy}^I)^2\right)\end{array}\right)} \quad ,$$

for the critical von Mises stress respectively yield strength with two different nanoindenter stress distributions σ_{ij}^L resulting from the pure normal loading $\sigma_{ij}^L=\sigma_{ij}^{normal\,load}$ and the mixed loading experimental setup $\sigma_{ij}^L=\sigma_{ij}^{mixed\,load}$. We have used the fact, that according to our approach (8) for the intrinsic stresses we can write the intrinsic stress field as $\sigma_{ij}^I=\sigma_{rr}^f*f_{ij}^I\left(x,y,z\right)\equiv\sigma_{rr}^f*f_{ij}^I$ with a suitable function f(x,y,z). Due to the linear independence of the two loading conditions we can now extract the intrinsic stress value σ_{rr}^f residing in the coating and the critical von Mises stress of an corresponding unstressed material ($\sigma_{rr}^f=0$), meaning the von Mises stress this unstressed material would require in order to reach its yield strength limit $\sigma_M=\sigma_M^{crit}$.

The above described analyzing procedures shall now be demonstrated on some very first experimental examples. The measurements have been performed by T. Chudoba from the company ASMEC using a so called UNAT measurement system [1] equipped with a lateral force unit (LFU) which can generate und measure lateral forces und displacements with the same resolution like common nanoindenters in normal direction.

Four samples with 3µm CrN-coatings on silicon have been investigated with different but known biaxial stresses. A detailed description of the intrinsic stress determination and the nanoindentation procedures will be published elsewhere [32]. At first, Young's modulus,

N. Schwarzer, About Intrinsic Stresses – their effects and measurement via indenter, publication 18 of the Saxonian Institute of Surface Mechanics, online at www.siomec.de/pub/2007/001

contact@siomec.de   www.siomec.de

hardness H and yield strength Y have been determined using classical normal nanoindentation together with the concept of the effectively shaped indenter. The results are given in table 1.

Table 1: **Results of the classical Berkowich nanoindentation experiments for four different samples at 3 different loads. The yield strength "mixed Y" has been extracted from the experimental data by applying the method of the effective indenter [12]. The word "mixed" means, that the yield strength has not been corrected with respect to the intrinsic stresses.**

Sample No.	intr. Stresses GPa	F mN	Hc µm	H GPa	dH GPa	mixed Y GPa	E GPa	dE GPa	ny
1		4,9948	0,151	5,83	0,42	6,13	287,9	29,5	0,25
1	-0,09	29,976	0,378	6,48	0,18	6,71	280,3	13,0	0,25
1		99,99	0,675	7,24	0,14	7,32	238,0	6,2	0,25
2		4,9974	0,090	14,71	0,93	15,45	286,8	19,5	0,25
2	-1,1	29,989	0,245	15,06	0,56	15,60	268,1	11,7	0,25
2		99,997	0,457	15,39	0,26	15,57	234,9	4,5	0,25
3		4,996	0,083	17,00	5,85	15,60	265,5	91,3	0,25
3	-1,9	29,964	0,215	19,16	2,48	19,02	286,5	38,0	0,25
3		99,998	0,416	18,47	0,62	18,00	265,8	9,8	0,25
4		4,9845	0,092	14,19	2,38	14,45	273,7	48,9	0,25
4	-1,2	29,984	0,255	13,85	0,86	14,62	279,1	25,0	0,25
4		99,992	0,460	15,20	0,64	15,52	246,0	12,6	0,25

Table 2: **Lateral force measurement - no tilting moment taken into account. Results of the mixed normal and lateral load nanoindentation experiments with a 6µm diamond sphere for four different samples. The yield strength Y, the critical tensile stress XX and non-critical von Mises maxima σ_M have been extracted from the experimental data by applying the method of the effective indenter [12]. The word "mixed" means, that the yield strength has not been corrected with respect to the intrinsic stresses, while "correct" stands for the corresponding material parameters without intrinsic stresses. Here we need to point out that, because a second linear independent indentation was not applicable for the determination of yield strength and intrinsic stresses separately, the evaluation of the correct σ_M was performed with the known intrinsic stress values (known from X-ray scattering measurements [32]) as they are given in table 1.**

No.	p_0 mN	mixed Y GPa	correct Y GPa	p_1 mN	T_x mN	mixed σ_M GPa	correct σ_M GPa	correct σ_M on surface in GPa	mixed XX on surface in GPa	correct XX on surface in GPa
1	250	7,33	7,24	175	11	5,56	5,48	4,81	3,37	3,28
2	250	15,68	14,86	175	6	12,38	11,49	9,34	5,99	4,89
3	250	18,31	16,71	175	7,5	14,53	13,47	11,06	7,77	5,87
4	250	14,52	13,75	175	9	11,49	10,57	9,16	6,51	5,31

N. Schwarzer, About Intrinsic Stresses – their effects and measurement via indenter, publication 19 of the Saxonian Institute of Surface Mechanics, online at www.siomec.de/pub/2007/001

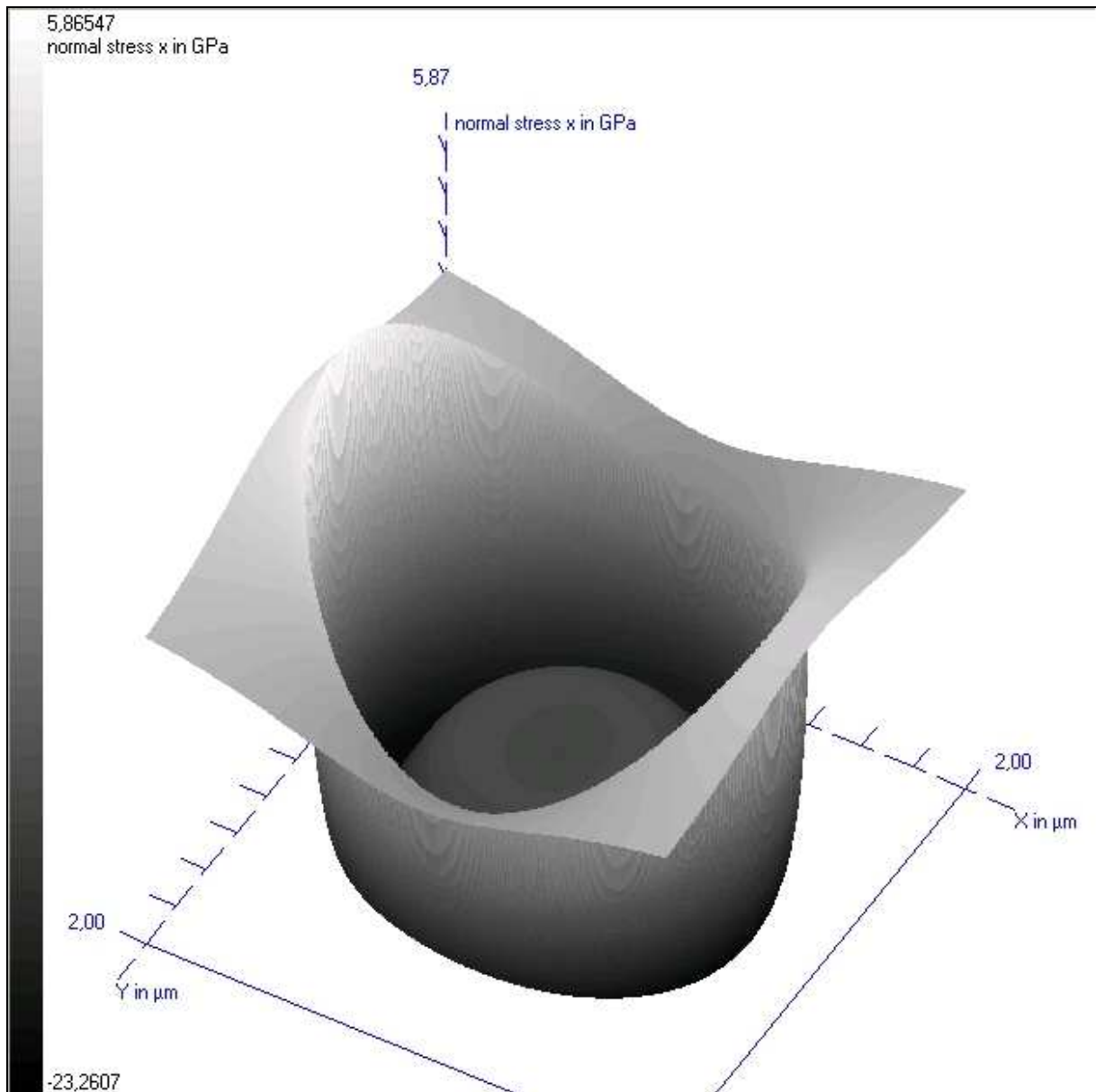contact@siomec.de   www.siomec.de

Fig. 11: **Resulting normal lateral stress in x-direction for sample 3 under combined load in normal (175mN) and lateral (7.5mN) direction (see table 2) using a 6μm diamond sphere – real experiment.**

From the relatively small differences between the yield strength values for the three different loads one can deduce that the coatings were quite homogenous. This especially holds for sample 2. According to our measurement procedure as proposed above we would require a combined normal and lateral measurement regime. This was in fact done with all samples but, in order to avoid discussions about the possible effects of the Berkowich edges, all measurements were also performed with a 6μm spherical indenter in the plastic regime. We detected similar results for both types of indenters, but in order to avoid overloading the paper with experimental results, we restrict the presentation here to the spherical indents. A more comprehensive presentation will be published elsewhere [32]. The maximum load p_0 was chosen to be 250mN and the lateral load circle was started at a $p_1=0.7*p_0$. The detected critical lateral loads t_x are presented in table 2. Unfortunately the samples (seemingly → see 6.1.1) appeared to produce failure due to surface fracture, which did not provide the necessary second linear independent measurement for the yield strength as it would be required for the determination of the intrinsic stress. Nevertheless, the "mixed" and the corrected values for

N. Schwarzer, About Intrinsic Stresses – their effects and measurement via indenter, publication 20
of the Saxonian Institute of Surface Mechanics, online at www.siomec.de/pub/2007/001
contact@siomec.de   www.siomec.de

yield strength and critical tensile surface stress XX (see table 2) show clearly the importance of the knowledge of the intrinsic stresses. The values for yield strength and critical tensile surface stress XX have been determined by the use of the "concept of the effective indenter for layered materials" as presented for example in [16, 17] and briefly described above. We find that without taking into account intrinsic stresses, especially the critical tensile stresses would be severely overestimated for the samples 2, 3 and 4. Figure 11 shows the normal stress in x-direction in the moment of critical mixed normal (p_1=175mN) and lateral loading (t_x=7.5mN) for the sample 3. The huge influence of the rather small lateral load, compared to the normal one, is caused by the fact that the indenter must be considered as tilted towards the sample surface within the lateral loading process.
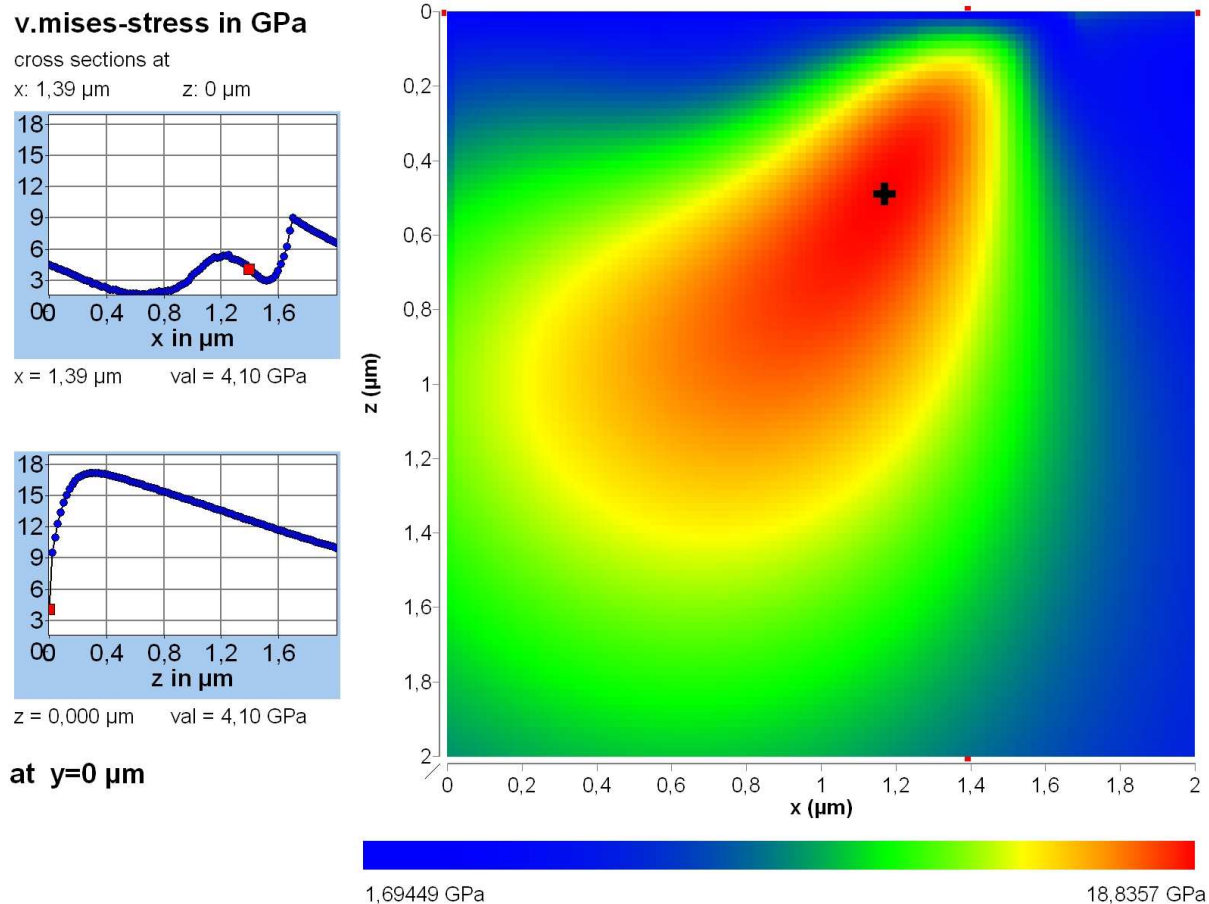

Fig. 12: **Resulting v. Mises stress in the x-z-plane for sample 3 under the combined load in normal direction (175mN), lateral (7.5mN) and indenter tilting (M_t=38.1mN, see table 3) using a 6µm diamond sphere. The stress is evaluated for the moment of beginning inelastic behaviour. The maximum (cross within the contour plot) almost perfectly agrees with the previously found yield strength Y (c.f. table 3).**

6.1.1. The dramatic effect of a tilting indenter shaft

Apart from the possibility that those coatings in fact might have shown failure due to surface fracture, there is also another possible explanation. In our case of lateral loading experiments all the evidence (limited lateral stiffness and comparison with other – known - results) seems to point to a slightly tilted indenter shaft. Assuming the resulting tilting moment of linear character, we simply postulate a tilting load with the dimension of a force M_t as:

$$M_t = const * T_x .$$ (17)

By using one of our samples (sample number 2 in table 2 and 3) as calibrator, we are able to determine *const*. This was simply done by looking for the tilting load necessary to produce the required additional von Mises stress in order to reach the yield strength Y. Now we can evaluate the resulting tilting angle δ for all samples and mixed load indentations by means of the following formula [22]

$$\delta = \frac{3*H*\alpha}{4a^2\left(1+\vartheta^2\right)}\left[\frac{M_t}{\vartheta}-T_x\right]; \quad H = \frac{1-v^2}{\pi E}; \quad \alpha = \frac{1-2v}{2\left(1-v\right)}; \quad \vartheta = \frac{\pi}{2}\ln\left[3-4v\right]. \quad (18)$$

The results are given in table 3. With M_t and δ known, we reevaluated the von Mises stresses for all samples and then obtained almost perfectly the von Mises stress maxima found to be critical in the previous purely normal nanoindentation experiments. This, together with the additional information that within this loading range the typical tilting angle would lay below 0.1° (found with well defined homogeneous samples), makes it almost certain that indeed a small but non-negligible tilting of the indenter has taken place here. The huge influence of very small tilting angles can bee seen in figure 12, where for sample 3 a very small angle of only 0.0656° already provides a rather influential tilting moment. It can also be concluded that by finding an other way to determine the tilting angle or the proportionality constant *const*, intrinsic stress and yield strength could be measured directly by the means of a combination of normal and mixed loading procedures. This directly follows from the excellent agreement of the expected Y and the evaluated von Mises stress (c.f. table 3).

A very detailed demonstration of how to perform the evaluation is given in the appendix.

Table 3: **Lateral force measurement - tilting of indenter shaft now taken into account. Results of the mixed normal and lateral load nanoindentation experiments with a 6μm diamond sphere for four different samples. By contrast to the results given in Table 2 now a rather small but very "influential" tilting of the indenter has been taken into account thereby using sample 2 for linear calibration of tilting load of all other indents (see text). The yield strength Y and the now critical von Mises maxima σ_M have been extracted from the experimental data by applying the method of the effective indenter [12]. The word "mixed" means, that the yield strength has not been corrected with respect to the intrinsic stresses, while "correct" stands for the corresponding material parameters without intrinsic stresses.**

No.	p_0	mixed Y	correct Y	p_1	T_x	tilting load	tilting angle	mixed σ_M	correct σ_M
	mN	GPa	GPa	mN	mN	mN	in grad °	GPa	GPa
1	250	7,33	7,24	175	11	56,0	0,0377	7,35	7,27
2	**250**	**15,68**	**14,86**	**175**	**6**	**30,5**	**0,0470**	**15,99**	**14,86**
3	250	18,31	16,71	175	7,5	38,1	0,0656	18,83	16,79
4	250	14,52	13,75	175	9	45,8	0,0658	14,89	14,11

6.2. Incorporation of torque - maintaining the symmetry of revolution

We now introduce the hypothetic indentation experiment with combined normal and torque loading. We see (table 4) that we can either reach the moment of beginning plastic flow (samples 1, 3 and 4) without surface fracture, or produce surface fracture again but at a non-critical von Mises stress. If we were able to measure torque and angle of revolution and would also detect the moments of beginning inelastic behavior, we could evaluate not only the correct value of critical stress (not mixed up with the intrinsic stresses) for the failure mechanism in question, but also could extract the intrinsic stress itself.

This means an indenter with a revolution force and measurement system for the torque angle around the axis of indentation appears to be quite desirable.

Table 4: Results of hypothetic mixed normal and rotation nanoindentation experiments with a 6µm diamond sphere for four different samples. The torque load (defined due to

$$M_{ROT} = \int_0^a \sigma_{\theta z}(r, z=0) dr \Bigg/ \left[\int_0^a \left(\sum_{n=1}^N r^{2n} \right) \sqrt{a^2 - r^2} dr \right]$$

) has been chosen such that the maximum von Mises stress σ_M is slightly bigger than the critical one. The tensile stress maxima σ_{xx} show, that except for sample 2 the critical von Mises maxima Y can be reached under mixed loading conditions without producing surface fracture. The word "correct" stands for the corresponding material parameters and stress values without intrinsic stresses (c.f. Table 2).

Sample No.	p₀ MN	correct Y GPa	p₁ mN	M_ROT mN	correct σ_M GPa	correct σ_M on surface in GPa	correct σ_xx on surface in GPa
1	250	7,24	175	29,5	7,28	7,28	3,02
2	**250**	**14,86**	**175**	**26,0**	**14,86**	**14,86**	**5,36**
2	**250**	**14,86**	**175**	**23,2**	**13,55**	**13,55**	**4,89**
3	250	16,71	175	27,3	16,71	16,71	5,86
4	250	13,75	175	26,7	13,77	13,77	5,11

7. Conclusions

It has been shown that critical stresses for distinct mechanical surface failure mechanisms and intrinsic stresses residing in the material's surface could be separately determined by the means of depth sensing nanoindetnation experiments with additional lateral load components. Within the paper, lateral and rotating loads have been investigated. While the combined normal and lateral load could be already realised with the help of a UNAT nanoindentation system, the rotating load is still rather hypothetic. Mixed normal and lateral loading procedures were used for the determination of yield strength and either intrinsic or critical tensile stress for surface fracture or similar surface damage sensitive to tensile stresses. It became clear that the tilting of the indenter is a very important factor which must be taken into account during the analysing of the indentation data.

It has further been shown how intrinsic stresses influence the resulting stress distribution of additional contact loads and the resulting load carrying capacity. The investigation has been performed for examples of homogenous half spaces, layered materials with monolithic and functionally graded coatings. In addition, the use of certain defects for the modelling of more complex intrinsic stress distributions or as stresses being residuals from former loading situations, has been considered.

Acknowledgment

N. Schwarzer, About Intrinsic Stresses – their effects and measurement via indenter, publication of the Saxonian Institute of Surface Mechanics, online at www.siomec.de/pub/2007/001

contact@siomec.de   www.siomec.de

23

Appendix - How to measure intrinsic stresses via nanoindentation – an example

Dr. rer. nat. habil. Norbert Schwarzer
Sächsisches Institut für Oberflächenmechanik SIO
Am Lauchberg 2
04838 Eilenburg
Tel. ++49(0)3423 656639
Fax. ++49(0)3423 656666
E-Mail: n.schwarzer@siomec.de
Internet: www.siomec.de

Abstract

In the following study the measurement an analysis of intrinsic stresses and yield strength via nanoindentation and their separation from each other will be elaborated using a specific example. The results for the intrinsic stresses are compared with those determined by other means. The agreement is excellent.

Introduction

Yield strength values obtained via nanoindentation are often flawed by the intrinsic stresses residing in the surfaces area of the samples in question. Within this study the procedure necessary to separate the intrinsic stresses and determine correct yield strength values is demonstrated on thin films with known biaxial intrinsic stresses.

In main paper (here referred as [A1]) the author has proposed the following measuring procedure:

1. The yield strength is determined using the method of the effectively shaped indenter as presented in [A1]. However, during unloading, the indenter is only drawn back to a distinct fraction of the maximum load p_0. This load shall be called p_1. The reader should note that p_1 must be chosen such that on the one hand there is "enough unloading curve" for the determination of the shape of the effective indenter, and on the other hand the load is still big enough in order to avoid strong and dominant inelastic unloading effects like e.g. unloading fractures. In addition, a p_1 close to p_0 also assures that the shape of the effective indenter only changes in an insignificant manner during unloading. We call the determined yield strength σ_M^{crit}. Here we now have to add the two elastic fields resulting from the intrinsic stresses σ_{ij}^I and the nanoindenter loading σ_{ij}^L. The von Mises stress can be written in the following form:

$$\sigma_M = \sqrt{\frac{1}{2}\left(\left(\sigma_{xx} - \sigma_{yy}\right)^2 + \left(\sigma_{zz} - \sigma_{yy}\right)^2 + \left(\sigma_{xx} - \sigma_{zz}\right)^2 + 6*\left(\tau_{xy}^2 + \tau_{xz}^2 + \tau_{zy}^2\right)\right)}$$

with $\sigma_{ij} = \sigma_{ij}^I + \sigma_{ij}^L$.

2. Now a slowly oscillating tangential load component t_x with increasing amplitude is added and the resulting lateral shift is measured. So we now have mixed load conditions and assume our - in step one determined - effectively shaped indenter acting with the combined load components p_1 and t_x onto the coating substrate compound.

3. The slowly oscillating tangential loading with increasing amplitude is monitored with very high resolution (as well as the static normal load and displacement, of course) until nonlinear

N. Schwarzer, About Intrinsic Stresses – their effects and measurement via indenter, publication of the Saxonian Institute of Surface Mechanics, online at www.siomec.de/pub/2007/001   24

contact@siomec.de   www.siomec.de

behavior can be detected. Thus, the value of maximum tangential load $t_x=t_{crit}$ or maximum lateral displacement u_σ is determined. Now we introduce the following assumption: The combined stresses add up to a mechanical stress field producing a maximum von Mises stress $\sigma_M = \sigma_M^{crit}$ somewhere within the investigated coating material.

4. With these two measurements and the resulting measured values p_0, p_1, the corresponding penetration depth, t_{crit} and u_σ we can construct two linear independent equations

$$\sigma_M^{crit} = \sqrt{\frac{1}{2}\begin{pmatrix} \left(\left(\sigma_{xx}^L - \sigma_{yy}^L + \sigma_{rr}^f\left(f_{xx}^I - f_{yy}^I\right)\right)^2 + \left(\sigma_{zz}^L - \sigma_{yy}^L + \sigma_{rr}^f\left(f_{zz}^I - f_{yy}^I\right)\right)^2\right) \\ + \left(\sigma_{xx}^L - \sigma_{zz}^L + \sigma_{rr}^f\left(f_{xx}^I - f_{zz}^I\right)\right)^2 \\ + 6*\left((\tau_{xy}^L + \sigma_{rr}^f f_{xy}^I)^2 + (\tau_{xz}^L + \sigma_{rr}^f f_{xz}^I)^2 + (\tau_{zy}^L + \sigma_{rr}^f f_{zy}^I)^2\right) \end{pmatrix}} \; ,$$

for the critical von Mises stress respectively yield strength with two different nanoindenter stress distributions σ_{ij}^L resulting from the pure normal loading $\sigma_{ij}^L = \sigma_{ij}^{normal\,load}$ and the mixed loading experimental setup $\sigma_{ij}^L = \sigma_{ij}^{mixed\,load}$. We have used the fact, that according to our approach (eq. (8) in [A1]) for the intrinsic stresses we can write the intrinsic stress field as $\sigma_{ij}^I = \sigma_{rr}^f * f_{ij}^I(x,y,z) \equiv \sigma_{rr}^f * f_{ij}^I$ with a suitable function f(x,y,z). Due to the linear independence of the two loading conditions we can now extract the intrinsic stress value σ_{rr}^f residing in the coating and the critical von Mises stress of a corresponding unstressed material ($\sigma_{rr}^f = 0$), meaning the von Mises stress this unstressed material would require in order to reach its yield strength limit $\sigma_M = \sigma_M^{crit}$.

The measurement and analyzing procedure in praxis

The above described analyzing procedures shall now be demonstrated on some very first experimental examples. The measurements have been performed by T. Chudoba and V. Linss from the company ASMEC using a so called UNAT measurement system [A2] equipped with a lateral force unit (LFU) which can generate und measure lateral forces und displacements with the same resolution like common nanoindenters in normal direction.

Four samples with 3µm CrN-coatings on silicon have been investigated with different but known biaxial stresses. A detailed description of the intrinsic stress determination and the nanoindentation procedures will be published elsewhere [A3]. Here we want to concentrate on the analysis of the experimental data. At first, Young's modulus, hardness H and yield strength Y have been determined using classical normal nanoindentation. The results are presented in [A1, table 1]. Now we want to follow the concrete procedure for one of those samples. For this we chose sample number 3 of [A1].

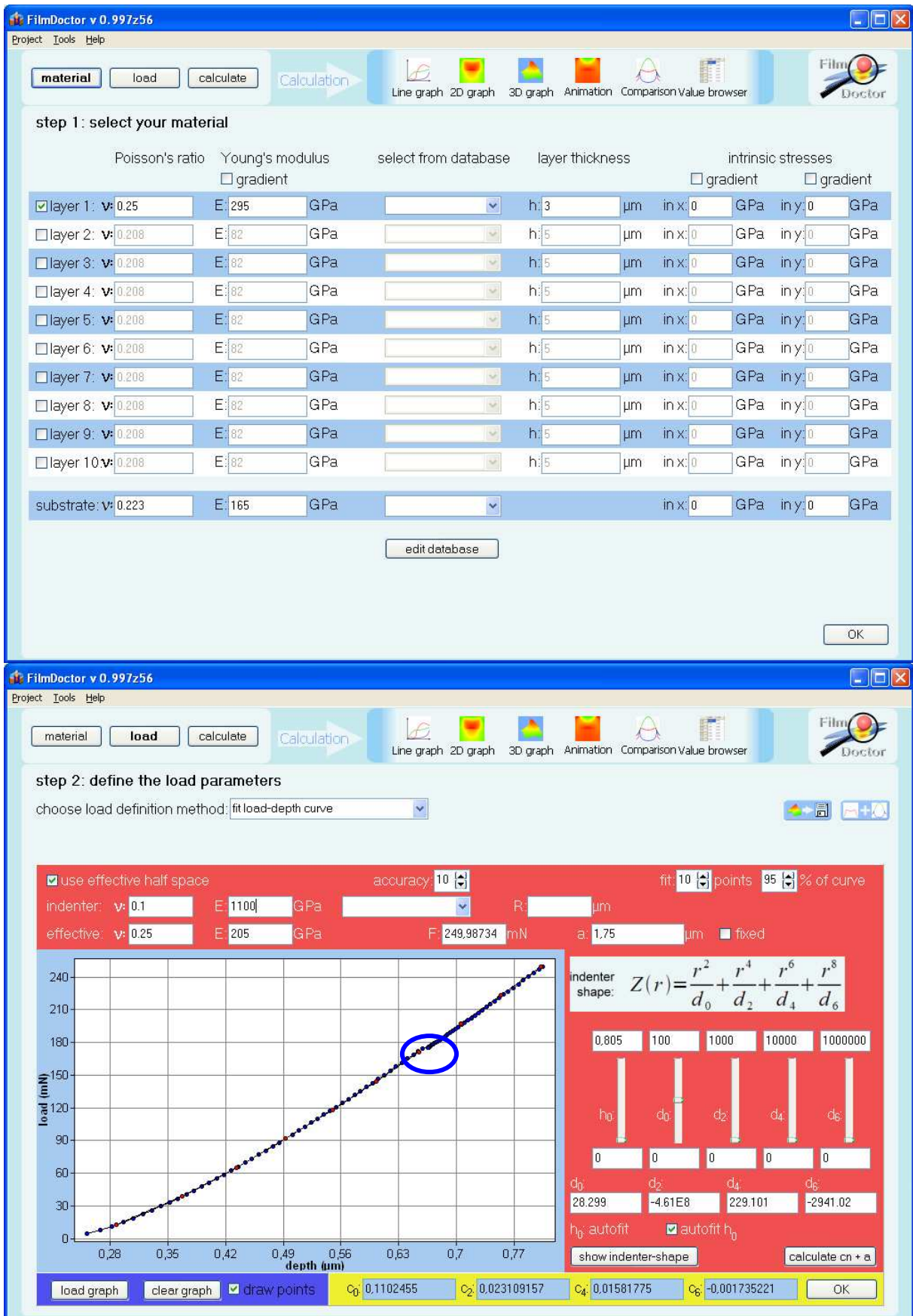# Analyzing procedure step I: pure normal indentation with max. load p_0

Fig. 1 and 2: Material data-input and fit of effective indenter to unloading curve

Using the software FilmDoctor, we first type in the material data Young's modulus, Poissons's ratio and thickness. As substrate we have silicon with a known Young's modulus of 165GPa and Poisson's ratio of 0.223. For the film we are estimating the Poisson's ratio and use the values determined by the means of the procedure described in [A4]. Now we chose "fit load-depth-curve" from the load definition page, load the indentation curve and fit a paraboloid indenter to the same. The fit can be done by hand or automatically. The next step is the evaluation of the elastic field of the effective indenter in the moment of beginning unloading (maximum load p_0). So, after setting up the parameters for the calculation (fig. 3).
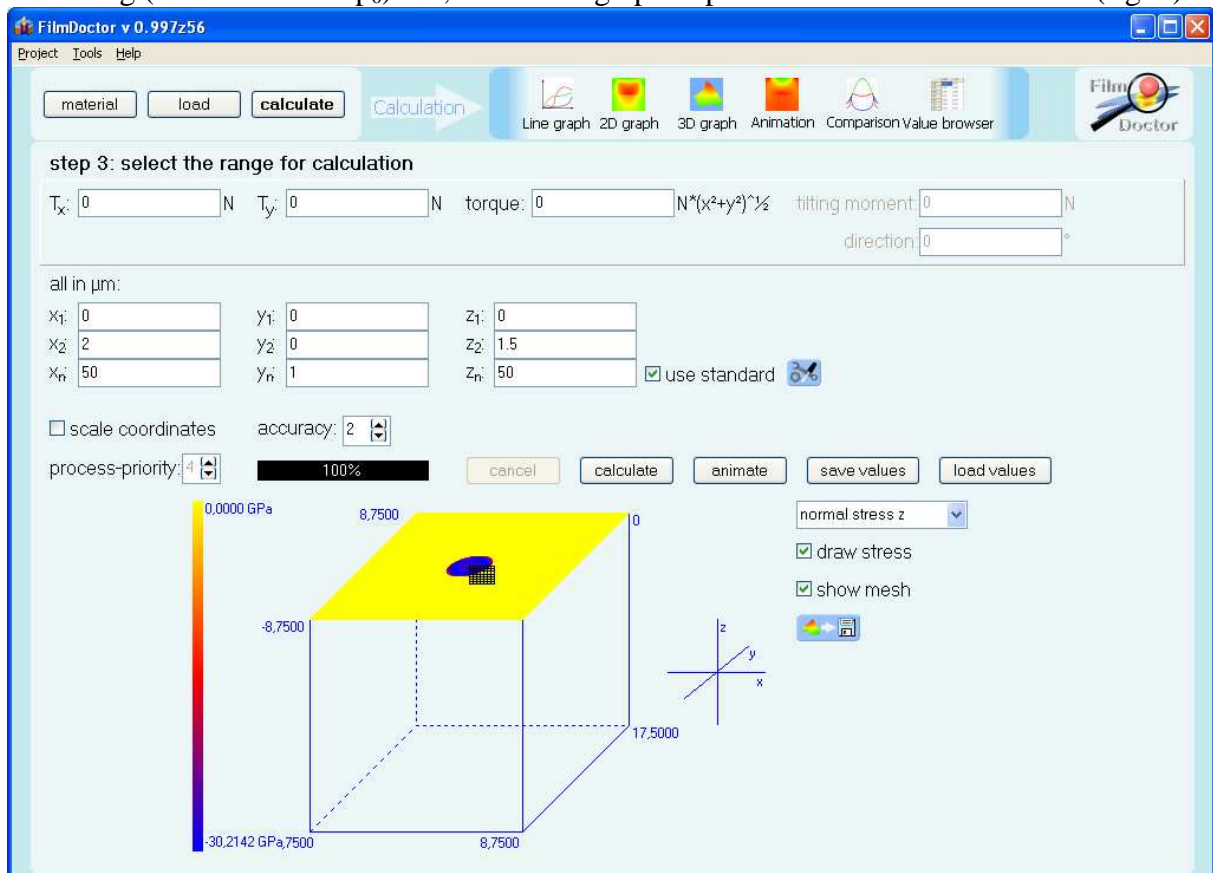

Fig. 3: Setting up the calculation-parameters and starting the evaluation

We find the von Mises Maximum (fig. 4 with 18.8357GPa), which is still mixed with the yet unknown intrinsic stress.
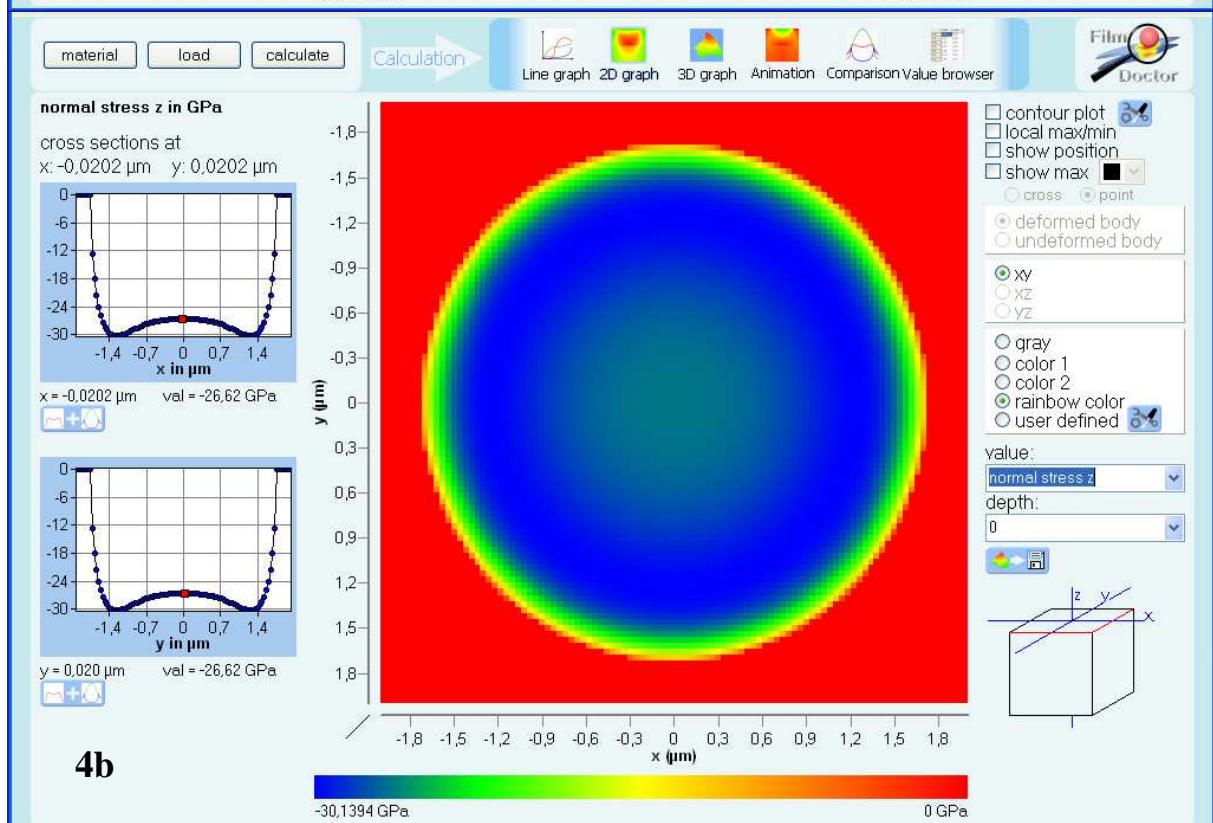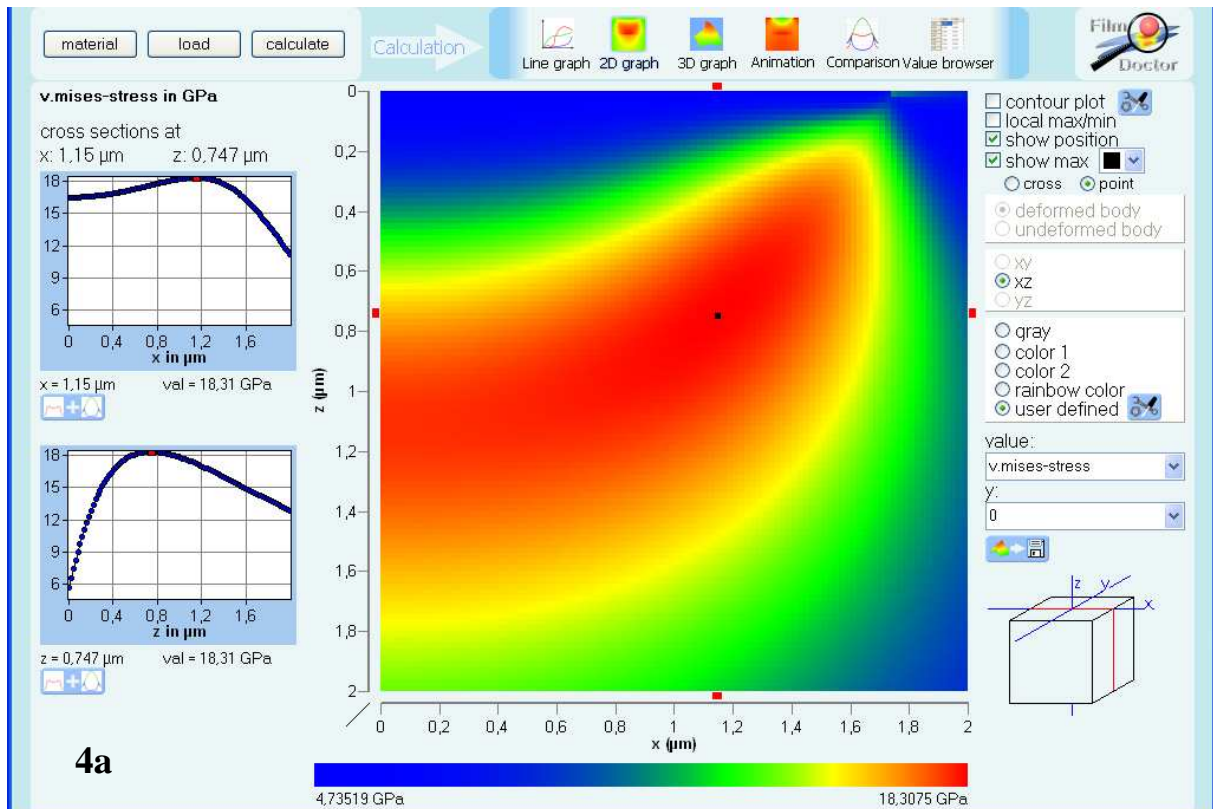
Fig. 4a: Resulting von Mises stress for the contact parameters given in fig. 2 at max. load p_0.
Fig. 4b: As the effective indenter produces a rather non-Hertzian normal surface pressure distribution (normal stress z), the von Mises maximum is to be found outside the axis of indentation.

Analyzing procedure step II: mixed normal and lateral indentation with maximum load 0.7*p_0

Now we reduce the normal load to 0.7*p_0 and start the lateral loading of the sample surface until again plastic flow respectively any other inelastic behavior can be observed. As effective indenter we either determine the new one for the reduced load by again fitting a paraboloid to the unloading curve after the lateral loading procedure or simply use the effective indenter from step I at reduced normal load. However, the latter is only possible when the surface shape of the inelastically deformed surface is not significantly changed during the lateral loading procedure, which would result in an incontinuity of the unloading curve at the position of the introduced load (blue ellipse in fig. 2).

The author wants to point out here, that instead of a lateral load also inclined normal indention should allow to obtain a second measurement sufficiently linear independent from the pure normal loading. However, this would require a well calibrated equipment clearly assigning lateral t_x and tilting load M_t to the indenter inclination and normal load.

Analyzing procedure step III: evaluation of the von Mises stress for the mixed normal and lateral indentation with normal load 0.7*p_0 and lateral load t_x

We assume that at a normal load of 0.7*p_0 and a lateral load t_x inelastic behavior has been detected. Now we evaluate the von Mises stress for this mixed loading situation. As described in [A1] we have to take into account, that usually lateral or inclined indentation also produces indenter tilting. In the example considered here we found the following loading conditions:
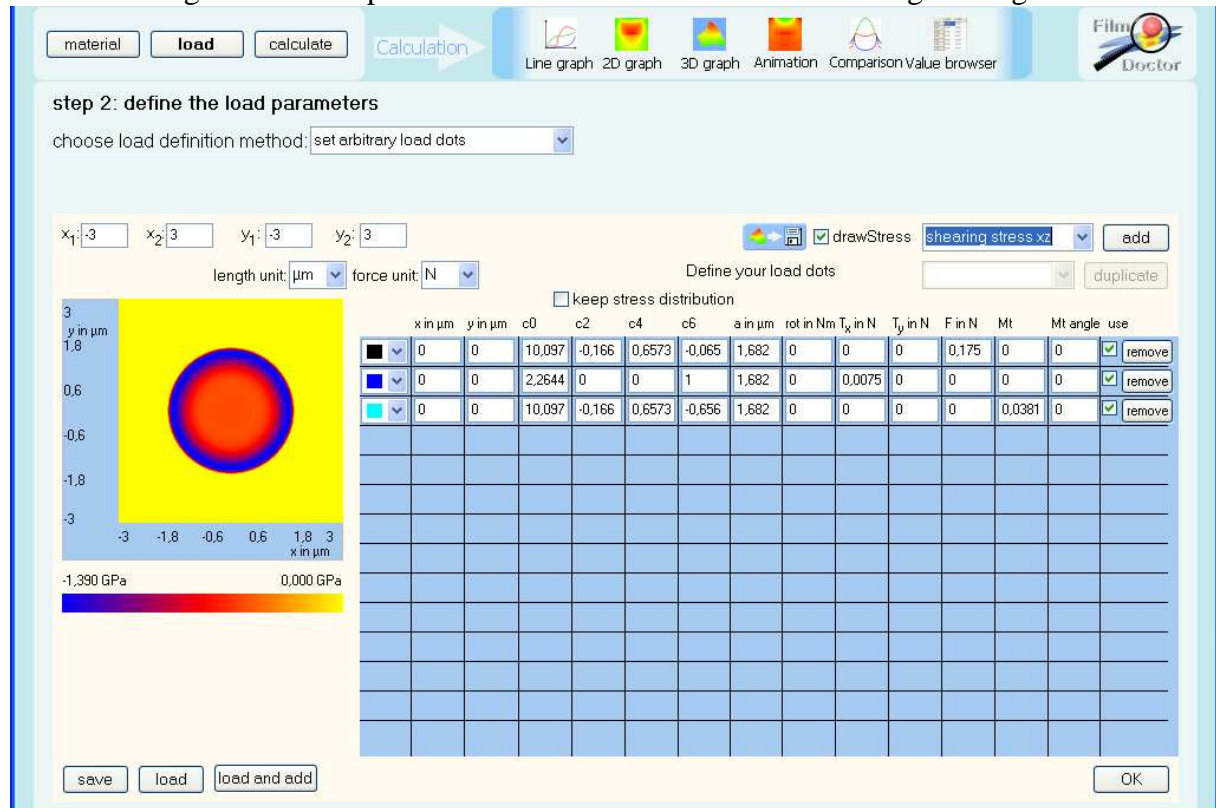

Fig. 5: Parameters for the mixed load evaluation
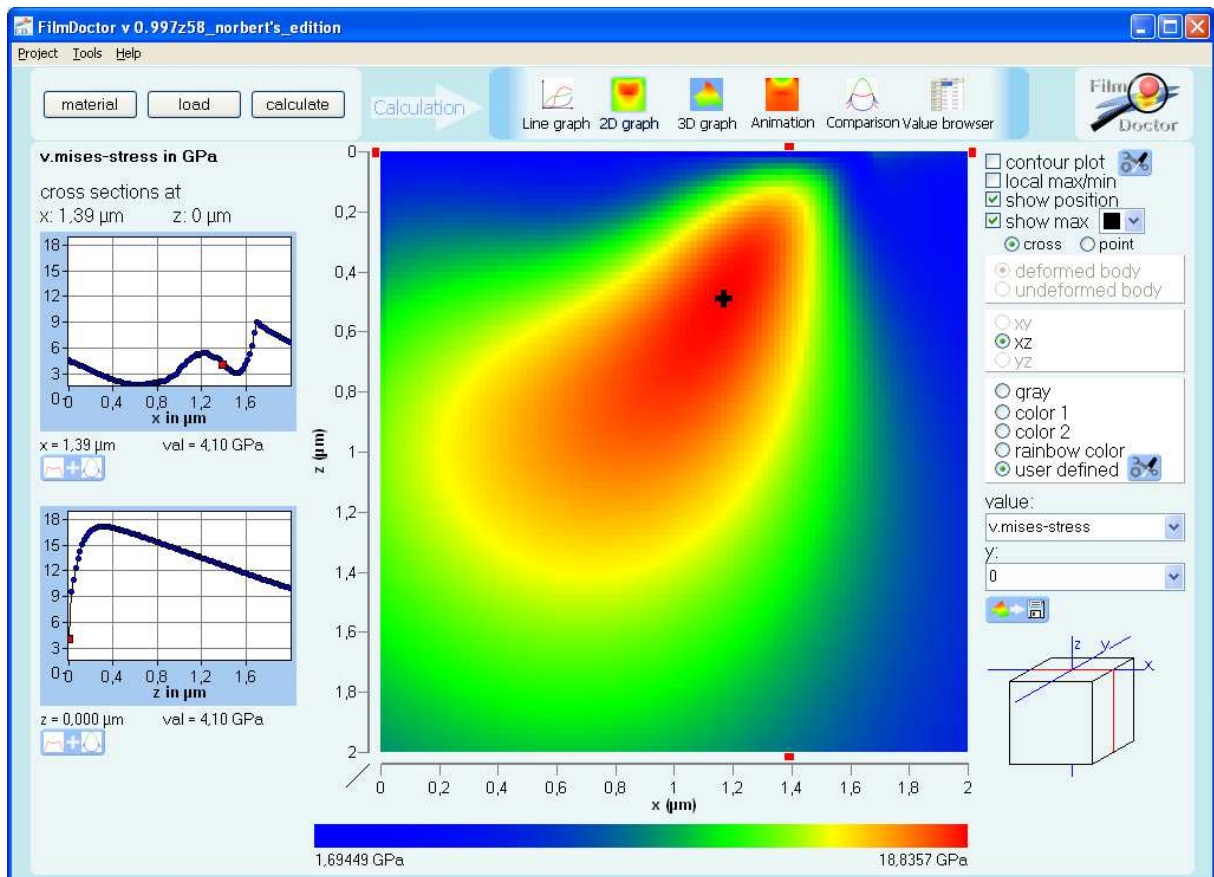
Fig. 6: Resulting von Mises stress for the mixed load situation.

Analyzing procedure step IV: evaluation of the "pure" yield strength and the intrinsic stress

From the equations given above we can easily obtain a formula for the intrinsic film stress σ_{rr}^f:

N. Schwarzer, About Intrinsic Stresses – their effects and measurement via indenter, publication 30 of the Saxonian Institute of Surface Mechanics, online at www.siomec.de/pub/2007/001

contact@siomec.de   www.siomec.de

$$\sigma_{rr}^{f} = \cfrac{
\begin{aligned}
&-6\left(f_{xy}^{I}\tau_{xy}^{L}+f_{xz}^{I}\tau_{xz}^{L}+f_{yz}^{I}\tau_{yz}^{L}\right)+f_{xx}^{I}\left(-2\sigma_{xx}^{L}+\sigma_{yy}^{L}+\sigma_{zz}^{L}\right)\\
&+f_{yy}^{I}\left(-2\sigma_{yy}^{L}+\sigma_{xx}^{L}+\sigma_{zz}^{L}\right)+f_{zz}^{I}\left(-2\sigma_{zz}^{L}+\sigma_{yy}^{L}+\sigma_{xx}^{L}\right)\\
&\pm\sqrt{
\begin{pmatrix}
4\begin{pmatrix}f_{xx}^{I\,2}+f_{yy}^{I\,2}+3\left(f_{xy}^{I\,2}+f_{xz}^{I\,2}+f_{yz}^{I\,2}\right)\\ -f_{yy}^{I}f_{zz}^{I}+f_{zz}^{I\,2}-f_{xx}^{I}\left(f_{yy}^{I}+f_{zz}^{I}\right)\end{pmatrix}\\
*\begin{pmatrix}\sigma_{M}^{crit\,2}-\sigma_{xx}^{L\,2}-\sigma_{yy}^{L\,2}-3\left(\tau_{xy}^{L\,2}+\tau_{xz}^{L\,2}+\tau_{yz}^{L\,2}\right)\\ +\sigma_{yy}^{L}\sigma_{zz}^{L}-\sigma_{zz}^{L\,2}+\sigma_{xx}^{L}\left(\sigma_{yy}^{L}+\sigma_{zz}^{L}\right)\end{pmatrix}\\
+\begin{pmatrix}-6\left(f_{xy}^{I}\tau_{xy}^{L}+f_{xz}^{I}\tau_{xz}^{L}+f_{yz}^{I}\tau_{yz}^{L}\right)+f_{xx}^{I}\left(-2\sigma_{xx}^{L}+\sigma_{yy}^{L}+\sigma_{zz}^{L}\right)\\ +f_{yy}^{I}\left(-2\sigma_{yy}^{L}+\sigma_{xx}^{L}+\sigma_{zz}^{L}\right)+f_{zz}^{I}\left(-2\sigma_{zz}^{L}+\sigma_{yy}^{L}+\sigma_{xx}^{L}\right)\end{pmatrix}^{2}
\end{pmatrix}}
\end{aligned}
}{
2\begin{pmatrix}f_{xx}^{I\,2}+f_{yy}^{I\,2}+3\left(f_{xy}^{I\,2}+f_{xz}^{I\,2}+f_{yz}^{I\,2}\right)\\ -f_{yy}^{I}f_{zz}^{I}+f_{zz}^{I\,2}-f_{xx}^{I}\left(f_{yy}^{I}+f_{zz}^{I}\right)\end{pmatrix}
}. \tag{19}$$

Assuming now only biaxial stress one simply has to compare the expected value for the unstressed case with the measured one σ_{M}^{crit} and could evaluate σ_{rr}^{f} using equation (19), which can be dramatically simplified due to the fact that within the coating $f_{xx}^{I}=f_{yy}^{I}=1$ and all other $f_{ij}^{I}=0$.

$$\sigma_{rr}^{f}=\frac{-\sigma_{xx}^{L}-\sigma_{yy}^{L}+2\sigma_{zz}^{L}\pm\sqrt{4\sigma_{M}^{crit\,2}-3\left(\left(\sigma_{xx}^{L}-\sigma_{yy}^{L}\right)^{2}+3\left(\tau_{xy}^{L\,2}+\tau_{xz}^{L\,2}+\tau_{yz}^{L\,2}\right)\right)}}{2}. \tag{20}$$

So the two measurements provide us with two equations we can solve with respect to σ_{M}^{crit} and σ_{rr}^{f} [A5].

For the sample considered here we obtain σ_{M}^{crit} =16.6GPa and σ_{rr}^{f} =-2.03GPa, with the latter being in very good agreement with the value measured by other means (-1.9GPa, c.f. [A3]). By taking the biaxial intrinsic stress fixed to its directly measured value of σ_{rr}^{f} =-1.9GPa one would obtain two possible values for the yield strength, namely 16.79GPa in mixed loading and 16.71GPa in the pure normal loading case.

From the small difference of these two values and the considerations presented in [A5] one can easily deduce, that measurement of intrinsic stresses via nanoindenter requires a very high accuracy and well calibrated equipment. However, the procedure described here could also be used as a simple estimator for the maximum value the intrinsic stress can not exceed and thus, giving more precise error bars for the yield strength (respectively hardness) determined from nanoindentation data. This way big hardness or yield strength values only obtained due to huge intrinsic compressive stresses will not pass as absolute material properties. Such an information is of special importance when nanoindenter results from pure normal loading states are going to be used in applications with mixed loading conditions.

All evaluations have been performed using a special prototype of the software FilmDoctor [A6].

References of the Appendix:

[A1] N. Schwarzer, "Intrinsic stresses – Their influence on the yield strength and their measurement via nanoindentation", online-documents of the Saxonian Institute of Surface Mechanics, www.siomec.de/pub/2007/001

[A2] V. Linss, T. Chudoba, M. Karniychuk, F. Richter, Thin Solid Films, 494 (2006) 179-183.

[A3] T. Chudoba, N. Schwarzer, V. Linss, Thin Solid Films, to be submitted

[A4] N. Schwarzer: "Analysing system for the investigation of ultra-thin coatings – determination of their Young's modulus, hardness and yields strength using the method of the 'Effective Indenter'", online-documents of the Saxonian Institute of Surface Mechanics, www.siomec.de/doc/2007/001

[A5] N. Schwarzer, "Modelling of the mechanics of thin films using analytical linear elastic approaches", Habilitationsschrift der TU-Chemnitz 2004, FB Physik Fester Körper, published in the online-archive of the Technical University of Chemnitz available at: http://archiv.tu-chemnitz.de/pub/2004/0077

[A6] FilmDoctor: software package for the evaluation of the elastic field of arbitrary combinations of normal, rotating and lateral loads of the type $\sim r^n \sqrt{a^2 - r^2}$ (with n=0,2,4,6), available from the internet at: http://www.siomec.de/downloads (contact: service@siomec.de).

References:

[1] V. Linss, T. Chudoba, M. Karniychuk, F. Richter, Thin Solid Films, 494 (2006) 179-183.

[2] V. Linss, T. Chudoba, Determiation of the critical tensile stress of sapphire by spherical indentation with additional lateral forces, proceedings of the NANOMEC 2005, accepted for publication in Int. J. Mat. Res. (formerly Z. Metallkd.).

[1] C. Spaeth, M. Kuehn, T. Chudoba, F. Richter, "Mechanical properties of carbon nitride thin films prepared by ion beam assisted filtered cathodic vacuum arc deposition", Surf. Coat. Techn. 112 (1999)140-145.

[2] S. Finnie, W. Cheng, I. Finnie, J. M. Drezet, M. Gremaud, "The Computation and Measurement of Residual Stresses in Laser Deposited Layers", ASME J. Eng. Mat. Technol. 125, 3, 302-308.

[3] A. Hoger, "The elastic tensor of a residually stressed material", J. of Elasticity 31 (1993), 219-237.

[4] E. Suhir, "An Approximate Analysis of Stresses in Multilayered Elastic Thin Films", J. Appl. Mech., 55 (1988) 143.

[5] G. G. Stoney, "The tension of metallic films deposited by electrolysis", Proc. Royal Soc. London, A82 (1909) 172.

[8] M. Ohring, "The Materials Science of Thin Films", Academic Press, San Diego, CA, 1992, pp. 413.

[9] N. Schwarzer, F. Richter, "On the determination of film stress from substrate bending: STONEY´s formula and its limits", published in the online-archive of the Technical University of Chemnitz at: http://archiv.tu-chemnitz.de/pub/2006/0011.

[10] D. S. Stone, "Elastic rebound between an indenter and a layered specimen", J. Mater. Res., Vol. 13, No. 11, November 1998, 3207 – 3213.

N. Schwarzer, About Intrinsic Stresses – their effects and measurement via indenter, publication of the Saxonian Institute of Surface Mechanics, online at www.siomec.de/pub/2007/001   32

contact@siomec.de   www.siomec.de

[11] N. Schwarzer, "Modelling of the mechanics of thin films using analytical linear elastic approaches", Habilitationsschrift der TU-Chemnitz 2004, FB Physik Fester Körper, published in the online-archive of the Technical University of Chemnitz available at: http://archiv.tu-chemnitz.de/pub/2004/0077.

[12] N. Schwarzer, "Elastic Surface Deformation due to Indenters with Arbitrary symmetry of revolution", J. Phys. D: Appl. Phys., 37 (2004) 2761-2772.

[13] H. Hertz, Hertz's Miscellaneous Papers; Chs. 5 and 6. Macmillan, London, U.K., 1896

[14] N. Schwarzer, The extended Hertzian Appraoch for lateral loading, online archive of the Technical University of Chemnitz: http://archiv.tu-chemnitz.de/pub/2006/0015; see also N. Schwarzer, L. Geidel, Automated Analysing of Thin Film Nanoindentation Data Using the Concept of the Effectively Shaped Indenter, proceedings of the ICMCTF 1 – 5 May 2006 in San Diego, California, USA, accepted June 2006.

[15] N. Schwarzer, G. M. Pharr: „On the evaluation of stresses during nanoindentation with sharp indenters", proceedings of the ICMCTF 2004 in San Diego, California, USA, also in Thin Solid Films, Vol. 469-470C pp. 194-200.

[16] N. Schwarzer, T. Chudoba, G. M. Pharr: „On the evaluation of stresses for coated materials during nanoindentation with sharp indenters", Surf. Coat. Technol, Vol 200/14-15 pp 4220-4226, doi:10.1016/j.surfcoat.2005.01.011.

[17] N. Schwarzer, T. Chudoba, F. Richter: „Investigation of ultra thin coatings using Nanoindentation", Surface and Coatings Technology, Vol 200/18-19 pp 5566-5580, online at doi: http://dx.doi.org/10.1016/j.surfcoat.2005.07.075.

[18] N. Schwarzer: "The extended Hertzian theory and its uses in analysing indentation experiments", Phil. Mag. 86(33-35) 21 Nov - 11 Dec 2006 5153 – 5767, Special Issue: "Instrumented Indentation Testing in Materials Research and Development"

[19] N. Schwarzer: "Arbitrary load distribution on a layered half space", ASME Journal of Tribology, Vol. 122, No. 4, October 2000, 672 – 681.

[20] A. Bolshakov, G.M. Pharr, Mat. Res. Symp. Proc., Mat. Res. Soc., 189 (1997)

[21] N. Schwarzer, Short note on the effect of lateral displacement on the surface stress distribution for cone and sphere contact, Phil. Mag. special issue "Instrumented Indentation", accepted March 2006.

[22] V. I. Fabrikant, "Application of potential theory in mechanics: A Selection of New Results", Kluver Academic Publishers, The Netherlands, 1989.

[23] FilmDoctor: software demonstration package for the evaluation of the elastic field of arbitrary combinations of normal, rotating and lateral loads of the type $\sim r^n \sqrt{a^2 - r^2}$ (with n=0,2,4,6), available from the internet at: http://www.siomec.de/downloads (contact: service@esae.de).

[24] N. Schwarzer: "Coating Design due to Analytical Modelling of Mechanical Contact Problems on Multilayer Systems", Surface and Coatings Technology 133 –134 (2000) 397 – 402.

[25] V. Linss, N. Schwarzer, T. Chudoba, M. Karniychuk, F. Richter: "Mechanical Properties of a Graded BCN Sputtered Coating with VaryingYoung's Modulus: Deposition, Theoretical Modelling and Nanoindentation", Surf. Coat. Technol., 195 (2005) pp 287 - 297, doi:10.1016/j.surfcoat.2004.06.010.

[26] J. G. Swadener, B. Taljat, G. M. Pharr, "Measurement of residual stress by load and depth sensing indentation with spherical indenters", J. of mat. Research, Vol 16, No. 7, 2001, 2091-2102.

N. Schwarzer, About Intrinsic Stresses – their effects and measurement via indenter, publication of the Saxonian Institute of Surface Mechanics, online at www.siomec.de/pub/2007/001   33

contact@siomec.de   www.siomec.de

[27] B. Taljat, G. M. Pharr, "Thin Films: Stresses and Mechanical Properties VIII", edited by R. Vinci, O. Kraft, N. Moody, E. Shaffer II (Mater. Res. Soc. Symp. Proc. 594, Warrendale, PA 2000), p. 519.

[28] E. Coronel, M. Smid, U. Wiklund, S. Hogmark, "On the influence of residual stress on hardness and elastic modulus", talk given on the ICMCTF 2004 in San Diego, California, USA.

[29] B.S. Anantha Ram, J. Danckert, T.G. Faurholdt, "Computation of Young's modulus and residual stress of hard surface coatings on elasto-plastic substrates through indentation experiments, finite element (FE) Simulations and inverse modelling technique", talk given on the ICMCTF 2004 in San Diego, California, USA.

[30] G. M. Pharr, B. Bolshakov, "Understanding nanoindentation unloading curves", J. Mater. Res., Vol. 17, No. 10, Oct 2002.

[31] T. Chudoba, N. Schwarzer, V. Linss, F. Richter: „Determination of Mechanical Properties of Graded Coatings using Nanoindentation", Thin Solid Films (2004): 469-470C pp. 239-247.

[32] T. Chudoba, N. Schwarzer, V. Linss, Thin Solid Films, to be submitted.

N. Schwarzer, About Intrinsic Stresses – their effects and measurement via indenter, publication 34 of the Saxonian Institute of Surface Mechanics, online at www.siomec.de/pub/2007/001

contact@siomec.de   www.siomec.de